CAPITAL UNIVERSITY OF SCIENCE AND TECHNOLOGY,
ISLAMABAD

Numerical study of peristaltic flow of different shaped nanoparticles in curved channel with magnetic field effects

by

Shaukat Mahmood

A thesis submitted in partial fulfillment for the
degree of Master of Philosophy

in the
Faculty of Computing
Department of Mathematics

November 2017

Declaration of Authorship

I, Shaukat Mahmood, declare that this thesis titled, 'Numerical study of peristaltic flow of different shaped nanosize particles in curved channel with magnetic field effects' and the work presented in it are my own. I confirm that:

- This work was done wholly or mainly while in candidature for a research degree at this University.
- Where any part of this thesis has previously been submitted for a degree or any other qualification at this University or any other institution, this has been clearly stated.
- Where I have consulted the published work of others, this is always clearly attributed.
- Where I have quoted from the work of others, the source is always given. With the exception of such quotations, this thesis is entirely my own work.
- I have acknowledged all main sources of help.
- Where the thesis is based on work done by myself jointly with others, I have made clear exactly what was done by others and what I have contributed myself.

Signed: _____

Date: _____

"The roots of education are bitter but the fruit is sweet."

Aristotle

Abstract

In this dissertation, we study the peristaltic transport of nanofluids with effects of magnetic field. Three different geometries of nanoparticle namely bricks, cylinder and platelets are considered in our analysis. The flow geometry is considered as a curved artery to analyse the model for various biomedical applications. The main object is to find and analyse the numerical solution of the governing model subject to physically pragmatic boundary conditions. The linear ordinary differential equation is found and is solved by using finite difference mtthod. The study is concluded on the basis of the effects of nanoparticles shapes,megnatic parameter, the curvature of the artery on the axial velocity, heat sourse parameter, Grashof parameter, amplitude of the parastaltic wall. The streamlines in a curved channel with variation of different flow parameters are discussed with the help of graphical illustrations. This study inferred that the instantaneous flow characteristics are affected by the magnetic parameter and curvature parameter of the artery. It displays further that a magnetic field brings, the potential to control the flow of blood arteries, pressure rise and pressure gradient. It is also possible to bring down these parameters to any appropriate level by increasing/decreasing the degree of intensity of the magnetic field. Thus, this study throws adequate light towards the therapeutic purpose of external magnetic field in the clinical and medical care of hemodynamic diseases.

Acknowledgements

All praises to Almighty **Allah**, the creator of all the creatures in the universe, who has created us in the structure of human beings as the best creature. Many thanks to Him, who created us as a muslim and blessed us with knowledge to differentiate between right and wrong. Many many thanks to Him as he blessed us with the Holy Prophet, **Hazrat Muhammad (Sallallahu Alaihay Wa'alihi wasalam)** for Whom the whole universe is created. He (Sallallahu Alaihay Wa'alihi wasalam) brought us out of darkness and enlightened the way to heaven.

I express my heart-felt gratitude to my supervisor **Dr. Muhammad Sagheer** for his passionate interest, superb guidance and inexhaustible inspiration through out this investigation. His textural and verbal criticism enable me in formatting this manuscript.

I would like to acknowledge CUST to providing me such a favourable environment to conduct this research.

My debt of gratitude goes to all of my respectable teachers especially Dr.Shafqat Hussain and Dr.Rashid for their inspirational guidance. May Almighty Allah shower His choicest blessings and prosperity on all those who assisted me in any way during completion of my thesis.

Contents

List of Figures

List of Tables

Nomenclature

t	**time**
p	**pressure**
B	**magnetic field**
C_p	**specific heat**
R_e	**Reynolds number**
G_r	**Grashof number**
κ	**thermal conductivity**
M	**Hartmann number**
T_0	**wall temperature**
T	**local temperature**
S	**Cauchy stress tensor**
(u, v)	**velocity components**

Greek Symbols

ρ	**fluid density**
μ	**viscosity**
ν	**kinematic viscosity**
τ	**stress tensor**
ψ	**stream function**
θ	**dimensionless temperature**
δ	**wave number**
ϵ	**amplitude ratio**
α	**thermal diffusivity**
ρ	**density**
ϕ	**nanofluid volume fraction**
γ	**thermal expansion coefficient**
ξ	**heat absorption parameter**
θ	**dimensionless temperature**

DEDICATION

I dedicate this Sincere Effort to my dear ***Parents*** *and my elegant* ***Teachers*** *who are always source of Inspiration for me and their contributions are uncounted.*

Chapter 1

Introduction

Peristalsis accounts for pumping fluids that deals with the propagation of sinusoidal waves which enforces the food to protrude from mouth to esophagus. In the urinary system, peristaltic procedure occurs due to inadvertently muscular contractions of the ureteral wall which pumps the urine from kidneys to bladder through the ureters. In physiology, peristaltic phenomenon is an imminent adjective of smooth muscle contraction. The mechanism of peristalsis is instructive in a large number of biological schemes comprising blood flows and the maneuver of chyme in the gastrointestinal channel, circulation of blood in blood vessels and in the efferent ducts of the male genital tract. In the industrial field, the phenomenon of peristaltic pumping suggests various suitable applications such as transfer of sanitary fluids, blood pump in the heart, lung machine, etc. Keeping all above valuable applications in mind, mathematical analysis of peristaltic flows of Newtonian fluid models with immersion of different forms of Cu nanoparticles such as Brickes, Cylinders and Platelets are presented in this thesis. The problems are solved in dimensionless form with the help of numerical methods. The governing equations of motion are reduced under the implementation of low Reynolds number and long wavelength.

Yin and Fung [1] have analyzed the waves peristaltically in cylindrical tubes by taking a Newtonian fluid flow problem brought or induced by an axisymmetric proceed sinusoidally of tolerant amplitude imposed on the outer wall of a tube and considered the perturbation method for solution. They also revealed that if the mean pressure gradient approaches a certain positive critical value, the velocity diminishes to zero on the axis and relatively larger values of the mean pressure gradient will account for reverse flow in the fluid. After one year later, Burns and Parkes [2] have investigated the peristaltic flow of a viscous fluid in axial symmetric pipes and symmetrical channels with the approximations of long wavelength and low Reynolds number it solved by an asymptotic expansion, used for the stream function in powers of the amplitude ratio by assuming

the amplitude ratio to be small. They described the effects of pressure gradient in their work. Srivastava and Srivastava [3] analyses the caseof peristaltic movment of a fluid under the same coditions as taken in above studies. They distributed the study in three parts. In first part, they presented a solution for a fluid with variable viscosity in a tapered tube. In second part, the solution was applied for plane and axisymmetric geometry, while in third one, the solution is extended to model biological fluid problems. In the present century, the researchers are also keen to enhance the theoretical and experimental investigations of peristaltic flows as these flows have become essential part in the progress and development of biomedical and industrial fields. Afifi and Gad [4] have described the interaction of peristaltic flow with pulsatile magneto-fluid through a porous medium with a transverse magnetic field. Later on, Misra and Pandey [5] have presented the model for blood flow in peristaltic tube by considering blood is two-layer fluid. After a couple of years, Mekheimer [6] has investigated the peristaltic flow of blood under the effect of a magnetic field in a non-uniform channels with the conditions of along with long wavelength and low Reynolds number. Nadeem and Akbar [7] have observed the heat transfer effects on the peristaltic transporting of MHD viscous fluid with changing viscosity. They have obtained the exact solution for temperature profile and velocity field is achieved by an Adomian decomposition method (ADM) along with the numerical solutions as well.

In all above mentioned studies, the flow problems are considered in two dimensional geometries (tube/channels). However, the studies regarding the three dimensional peristaltic flows have a very little amount of literature due to the complexity of highly nonlinear partial differential equations which often occur for the case of non-Newtonian models in three dimensional geometries (channel/tube). Only a small number of researchers are keen to work on peristaltic flow problems which deal with the three dimensional investigation. Reddy et al. [8] have introduced the influence of lateral walls on peristaltic flow in a rectangular duct under the same theoretical restrictions as taken by the researchers in above mentioned studies. The experimental investigation has been taken into account by Aranda et al. [9] in which they presented the Stokesian peristaltic pumping in a three-dimensional tube with a phase shifted asymmetry. Two years ago, Mekheimer et al.[10] have made analysis regarding effect of lateral walls on peristaltic flow through an asymmetric rectangular duct. More recently, Akram et al. [11] have presented the flow in a wave frame of reference moving with the uniform velocity away from the fixed frame and peristaltic waves produced on the horizontal walls of a non-uniform rectangular duct are justified under lubrication approach. They have illustrated the graphical results for the flow phenomenon and also discussed the circulating bolus scheme. Some more studies on the topic of peristaltic flows of Newtonian and non-Newtonian fluids

are given in [12-17].

Nanotechnology has tremendous contribution has played in the industry since nanometer materials of dimension and cannot be compared physically and chemically. Animal blood, Water, oil, ethylene glycol are famous examples of base fluids utilized for the nanofluid occurrence. Enormous application of nanofluid is generally heat transfer, like fuel cells, microelectronics, hybrid-powered engines, pharmaceutical processes, chiller, domestic refrigerator, nuclear reactor coolant, grinding and space technology, etc [18, 19]. In the recent time, the interaction of nanoparticles phenomenon in peristaltic flows has become the core of attention for many researchers, engineers, mathematicians, modelers and scientists due to the wide range of applications of nanoparticles in the field of peristaltic pumping. Nadeem and Maraj [20] mathematically analyzed for peristaltic flow of nanofluid in a curved artery. They reduced the extremely nonlinear, partial differential equations by employing the wave frame transformation, low Reynolds number and long wave length assumptions. The peristaltic flow of a nanofluid in a non-uniform tube have been produced by Akbar et al. [21].

Chapter one is based on the brief introduction of peristaltic flows. The mathematical models of Newtonian fluids are presented.

In Chapter two, Basic definitions, governing equations and numerical schemes are also incorporated. Two-Phase Model Governing Equations, Law of conservation of momentum for two-phase nanofluid model, Energy equation for nanofluids, Thermophysical Properties of nanoparticles, Thermal Conductivity of nanoparticles and its mathematical expression that represents thermal conductivity of different types of nanoparticles and Methods for solutions.

In Chapter three, there is straight vertical tube is taken with outer wall moving sinusoidal The nanofluid comprising different geometries of nanoparticles, which is flowing in the tube under the effects of magnetic field.

In Chapter four, we considered a vertical curved tube whose outer wall moving peristallticaly. The immersion of different types of nanoparticles such as bricks, cylinders and platelets in the tube and these nanoaprticles are also exposed to the external magnatic filed to control the flow of fluid.

In Chapter five includes the conclusion of the work presented in this thesis. All the references used in this dissertation are listed in **Bibliography**.

Chapter 2

Basic definitions and governing Equations

This chapter is prepared to present basic definitions related to fluid mechanics and definitions of some dimensionless numbers and equations just for the description of the flow analysis presented in this dissertation.

2.1 Fluid

A fluid is defined as an isotropic substance, the individual particles of which deform continuously under the application of a shearing stress, no matter how small it is.

Rheology

It is study of Newtonian fluid and non-Newtonian flow under the influence of an applied stress.

Concept of Continuum

All matter is composed of discrete entities of atoms and molecules which contain voids not occupied by any matter. Through the concept of such voids, the matter is distributed discretely and not continuously. Continuum is the name of abstract model that

assumes matter is distributed continuously in the form of liquid or gas, and this model is simply referred as continuum which provides us with the information that each fluid property has a finite value at every point in a given continuum.

2.2 Classification of fluids

Inviscid fluid

The fluid with constant density and zero viscosity under different temperature and stress conditions is defined as inviscid fluid.

Viscous fluid

The fluid with constant density but having resistance to shear stress is known as viscous fluid. These fluids are divided in two different major groups: Newtonian and non-Newtonian fluids.

Newtonian and non-Newtonian fluids

A non-viscous fluids whose stress rate is linearly proportional to its strain rate at every point which means it obeys the Newtons law of viscosity. Such fluids do not resist deformation and flow freely. Example are gasoline, light-hydrocarbon oils, glycerin, sugar solutions, mineral spirits, silicone oils, water and gases such as air etc.
A fluid violating the linear Newtonian relation between shear rate and stress is known as non-Newtonianfluid. Such fluids do not have well defined viscosity. Its viscosity changes with the applied strain rate. These fluids satisfy the stress-strain relation in a non-linear manner. Examples are blood, ketchup, polymer solution and tooth paste etc.

2.3 Basic Concepts of Heat transfer

Heat and temperature

Temperature is the average kinetic energy where as heat is the total kinetic energy of all the fluid particles. Heat is that state of energy whose exchange can take place from one place to another subject to the temperature difference between the two systems.
If there are two bodies with different temperatures heat flows from high to low temperature. Such heat transfer take place by three basic methods describe below.

Conduction

It can be defined as the transfer of energy from the more energetic particles of substance to the neighboring less energetic ones as a result of the interaction between the particles with no movement of material. Conduction is only because of the collision of the molecules not due to the transfer of molecules. For solids, conduction plays an important role in the heat transfer.

Convection

It is the mode of heat transfer between a surface and the adjoining fluid that is in motion and it involves the combined effect of condition and fluid motion. Here heat transfer occurs due to the transfer of molecules.

Natural convection

If the fluid motion occurs as a result of the density difference produced by the temperature difference, the process is called natural or free convection. In case of free convection flow is generated by the body forces that occurs as the result of the density changes arising from the temperature changes in the whole fluid. These body forces are actually generated by pressure gradients imposed on the whole fluid. That most common source of this imposed pressure field is gravity. The body forces in this case are usually termed as buoyancy forces. Without the existence of gravity and thermal expansion coefficient, natural convection would not be possible.

Forced convection

Convection is called forced convection if the fluid is forced to flow over the surface by external means such as pump, fan or the air. The term forced convection is only applied to flows in which the effects of the buoyancy forces are negligible.

Mixed convection

When both forced and natural convection take place at the same time and contribute significantly to heat transfer, then it is called Mixed Convection.

Radiation

The energy transmitted by the matter in the form of electromagnetic waves is termed as radiation does not require a material in which to propagate and can travel through vacuum.

Specific Heat

It is defined as the amount of energy needed to increase the temperature of one kilogram by one degree Celsius.

Thermal conductivity

The measure of the tendency of a given material to conduct heat is known as its thermal conductivity. The dimension of thermal conductivity is $\left[ML/T^3\theta\right]$ and its unit is $kg.m/a^3k$.

Thermal diffusivity

It is defined as the ratio of heat conducted through the material to the heat stored per unit volume.

Mathematically it can be written as

$$\propto= \frac{K}{\rho C_p}$$

The dimension of the thermal diffusivity is $\left[L^2/T\right]$and its unit is m^2/s.

2.4 Dimensionless numbers

Reynolds number

The Reynolds number is a meaningful nondimensional quantity in fluid dynamics offer to helped and predict fluid flow regimes in various fluid flow patterns. It holds many important applications in fluid mechanic. It is denoted by Re and is mathematically written as

$$Re = \frac{\rho u L}{\mu}. \tag{2.1}$$

Grashof number

The Grashof number is a nondimensionl quantity in fluid mechanics and heat transfer which approximates the ratio of the buoyancy forces to viscous forecs applying on a fluid. This number is denoted by Gr and is mathematically written as

$$Gr = \frac{g\beta(T_0 - T_1)D^3}{\nu^2} \tag{2.2}$$

Wave number

The ratio of the width of the channel to the wavelength is called wave number. Usually it is denoted by the Greek symbol δ and is

$$\boldsymbol{\delta = \frac{2\pi \breve{a}}{\lambda}} \tag{2.3}$$

Where $\tilde{a}$ denotes the width of the channel and$\lambda$the wavelength.

2.5 Amplitude ratio

The ratio of wave amplitude of the peristaltic wall to the thicknesses of the pipes is called amplitude ratio. This number can be written as

$$\epsilon = \frac{\tilde{b}}{\tilde{a}} \tag{2.4}$$

2.6 Some fundamentals of peristaltic transport

Peristalic transport

Peristalsis is a symmetrical radial contraction or relaxation of along the length of a distensible tube with some material [22- 24].

Pumping

Pumping phenomenon is a characteristic feature of peristaltic transport. The operation of a pump of moving liquids from low pressures to high pressure under certain conditions is termed as pumping. We can briefly pumping further as:

Positive and negative pumping

The pumping is called positive or negative depending on weather the mean flow rate Q is positive or negative.

Adverse and favourable pressure gradient

If the pressure rise per wavelength (P_λ) is positive gradient is said to be adverse and favorable otherwise.

Peristaltic pumping

Here the flow rate is positive ($Q > 0$) and pressure rise is adverse ($P_\lambda > 0$).

Augmented pumping

It occurs when flow rate is positive ($Q > 0$) but in this case pressure rise is favorable ($P_\lambda < 0$).

Retrograde pumping

In this situation the flow rate is negative ($Q < 0$) and pressure rise is adverse ($P_\lambda > 0$).

Free pumping

In this case the flow rate is positive ($\theta > 0$) but pressure rise neither adverse nor favorable.
In words$P_\lambda = 0$.

Free pumping flux

The critical value of mean flow rate Q corresponding to $P_\lambda = 0$ is called free pumping flux.

Bolus

Volume of the fluid trapped with in closed streamlines is termed as bolus.

Trapping

The phenomenon of formation of bolus is known as trapping.

2.7 Fundamental equations

Continuity equation

This equation is derived by using the conservation law of mass which is defined as that the mass can neither be distorted. In mathematical form the continuity equation is the

absence of sources or sinks is expressed as follows

$$\frac{\partial \rho}{\partial t} + \nabla \cdot \left(\rho \tilde{\boldsymbol{V}}\right) = 0, \tag{2.5}$$

Where ρ is the fluid density , $\tilde{V} = (U, V, W)$ the velocity of the fluid and t is the time. The above equation for an incompressible fluid is reduced as

$$\nabla \cdot \tilde{\boldsymbol{V}} = 0. \tag{2.6}$$

The above forms of continuity indicate absence of sources/ sink in the control volume.

Equation of motion

This equation is resulted by the law of conservation of linear momentum and is expressed

$$\rho \frac{d\tilde{\boldsymbol{V}}}{dt} = \nabla \cdot \tilde{S} + \rho \mathbf{b}, \tag{2.7}$$

where **b** represent by the body force and $\tilde{S}$ represent the Cauchy stress tensor.
In case of curved channel when

$$\tilde{\boldsymbol{V}} = \left[\tilde{V}\left(\bar{X}, \bar{R}, \bar{t}\right), \tilde{U}\left(\bar{X}, \bar{R}, \bar{t}\right), 0\right], \tag{2.8}$$

the Navier-Stokes equation for curved channel are

$$\frac{\partial \tilde{V}}{\partial t} + \left(\tilde{\boldsymbol{V}} \cdot \nabla\right) \tilde{V} - \frac{\tilde{U}^2}{\bar{R} + \tilde{R}^*} = (\nabla \cdot \tilde{S})_{\bar{R}}, \tag{2.9}$$

$$\frac{\partial \tilde{U}}{\partial t} + \left(\tilde{\boldsymbol{V}} \cdot \nabla\right) \tilde{U} - \frac{\tilde{V}\tilde{U}^2}{\bar{R} + \tilde{R}^*} = (\nabla \cdot \tilde{S})_{\bar{X}}, \tag{2.10}$$

$$\tilde{\boldsymbol{V}} \cdot \nabla = \tilde{V} \frac{\partial}{\partial \bar{R}} + \frac{\tilde{U} \cdot \tilde{R}^*}{\bar{R} + \tilde{R}^*} \frac{\partial}{\partial \bar{X}}. \tag{2.11}$$

Here $\tilde{R}^*$ is the radius of the curved channel also we have neglected the body force term.

Energy equation

This equation results from the basic law of thermodynamics also called conservation law of energy and express that the increase in the system's internal energy of a thermodynamic system is similar to the quantity of heat energy included to the system excluded the quantity of energy wasted as an outcome of the work done by the system on the

surroundings. Mathematically,

$$\rho C_p \frac{dT}{dt} = \tilde{S} \cdot \left(\nabla \tilde{\boldsymbol{V}} \right) + \nabla \cdot (k \nabla T) \,. \tag{2.12}$$

Where C_p is the specific heat and k the thermal conductivity.

2.8 Two-Phase Model Governing Equations

Law of conservation of momentum for two-phase nanofluid model

This law gives the equation of momentum which for nanofluid is similar to that of usual Navier Stokes equations but in the presence of external forces which are due to heat of nanoparticles. So the Navier-Stokes equation for nanofluid in the presence of body forces take the following form [25]

$$\rho_{n\mathfrak{f}} \left(\frac{\partial \boldsymbol{V}}{\partial \mathfrak{t}} + \boldsymbol{V} \cdot \nabla \boldsymbol{V} \right) = -\nabla P + \mu_{n\mathfrak{f}} \nabla^2 \boldsymbol{V} + g (\rho\gamma)_{n\mathfrak{f}} (T - T_0) \,, \tag{2.13}$$

Where ρ_{nf} is the density, μ_{nf} is the viscosity.

Energy equation

$$\rho c_p \frac{dT}{dt} = K \nabla^2 \, T + Q_0, \tag{2.14}$$

k_{nf} is the thermal conductivity, γ_{nf} is the thermal expansion coefficient and $(\rho c_p)_{nf}$ is the heat capacitance.

Thermophysical Properties

Both fluid and solid characteristics are supposed to be constant. The constant α for Cu, $Al_2O_{3,}$, and T_iO_2 are directly taken from a curve-fit relations. The general model for nanofluid is shown in this section [26-27].

1. Density

$$\rho_{n\mathfrak{f}} = (1 - \phi) \, \rho_{\mathfrak{f}} + \phi \rho_s. \tag{2.15}$$

2. Specific Heat

$$(\rho c_p)_{n\mathfrak{f}} = \phi(\rho c_p)_s + (1-\phi)(\rho c_p)_{\mathfrak{f}}. \tag{2.16}$$

3. Thermal Expansion Coefficient

$$(\rho\gamma)_{n\mathfrak{f}} = \phi(\rho\gamma)_s + (1-\phi)(\rho\gamma)_{\mathfrak{f}}. \tag{2.17}$$

4. Viscosity

$$\mu_{n\mathfrak{f}} = \frac{1}{(1-\phi)^{5/2}}. \tag{2.18}$$

Thermal Conductivity

$$k_{nf} = k_{static} + k_{Brownian}, \tag{2.19}$$

$$\frac{k_{static}}{k_{\mathfrak{f}}} = \frac{(k_{np}+2k_{\mathfrak{f}}) - 2\phi(k_{np}+k_{\mathfrak{f}})}{(k_{np}+2k_{\mathfrak{f}}) + 2\phi(k_{np}+k_{\mathfrak{f}})}, \tag{2.20}$$

$$\frac{k_{static}}{k_{\mathfrak{f}}} = \frac{k_{np}+(1+m)k_{\mathfrak{f}} - \phi(1+m)(k_{np}-k_{\mathfrak{f}})}{k_{np}+(1+m)k_{\mathfrak{f}} + \phi(k_{np}-k_{\mathfrak{f}})}, \tag{2.21}$$

$$k_{Brownian} = 5\times10^4\gamma\phi\rho_{\mathfrak{f}}C_{p,\mathfrak{f}}\sqrt{\frac{kT}{2\rho_{n\mathfrak{f}}R_{np}}}f(T,\phi), \tag{2.22}$$

where $k = 1.3807\times10^{-23}J/K$ and γ is the fraction of the volume of liquid which transfer with a particle, here,

$$f(T,\phi) = \left(2.8217\times10^{-2}\phi + 3.917\times10^{-3}\phi\right)\left(\frac{T+273.15}{T_o+273.15}\right)$$

$$+\left(-3.0669\times10^{-2}\phi - 3.99123\times10^{-3}\phi\right). \tag{2.23}$$

Physical properties	Fluid phase (blood)	Cu	Al_2O_3	TiO_2
$Cp(J/kgK)$	3594	385	765	686.2
$\rho\ (kg/m3)$	1063	8933	3970	4250
$K\ (W/mK)$	0.492	400	40	8.9538
$\gamma\ \times\ 10-5(1/K)$	0.18	1.67	0.85	0.9

TABLE 2.1: Thermophysical properties of fluid and nanoparticles

Nanoparticles	Shape factor
$Cu - Bricks$	3.7
$Cu - \ Cylinders$	4.9
$Cu - Platelets$	5.7

TABLE 2.2: Copper- nanoparticle shape factor (m)

2.9 Solution Methodology

Most of the natural procedure can be effectual and properly elaborated microscopically, without considering the single attitude of atoms, molecules, electrons etc. The common characteristics like stress, pressure, deformation, density, velocity, temperature, concentration or electromagnetic field are modeled as by partial differential equations (PDEs) which deal with the formulation of many engineering and scientific problems.
In physical phenomena, PDEs (second order) occurred in three forms i.e., elliptic, parabolic or hyperbolic. The general form of a PDE of a function $U\left(x_1,\ x_2,\ x_3 \cdots,\ x_n\right)$ can be expressed as

$$\mathcal{F}\left(\begin{array}{c} x_1,\ x_2,\ x_3 \cdots,\ x_n,\ U,\ \frac{\partial U}{\partial x_1},\ \frac{\partial U}{\partial x_2},\ \frac{\partial U}{\partial x_3}, \cdots,\ \frac{\partial U}{\partial x_n},\ \frac{\partial^2 U}{\partial x_1 \partial x_1}, \\ \frac{\partial^2 U}{\partial x_1 \partial x_2},\ \frac{\partial^2 U}{\partial x_1 \partial x_3} \cdots,\ \frac{\partial^2 U}{\partial x_1 \partial x_n},\ \cdots \end{array}\right) = 0. \tag{2.24}$$

In the present thesis, emphasize will be devoted to the properties and solution of hyperbolic PDEs. The most common models of hyperbolic PDE are a wave equation. A wave equation can either be linear or nonlinear depending upon the nature of the physical problem. To work a linear PDE, several methods are usable in the literature; like method of separation of variable, Laplace and Fourier transform methods, Greens functions and Eigen function expansion methods etc. Although, solutions of nonlinear PDEs is not an easy task. The nonlinear PDEs have a less chances to have exact or closed form solutions. For that reason, one has to seek some approximate numerical or analytical techniques. However, the analytical solutions have more significance than numerical because they provide a way of checking the convergence and validity by getting number of approximate solutions either numerical or empirical [28]. There exists a number of analytical techniques which can solve nonlinear PDEs encountered in almost all branches of science and engineering. Some of them are listed as: perturbation method, homotopy analysis method, homotopy perturbation method, optimal homotopy method. But here, we will only explain the analytical and finite difference method which are employed in the subsequent chapters.
Consider the differential equation

$$\frac{d^2U}{dx^2} + A\left(x\right)\frac{dU}{dx} + B\left(x\right)U = D\left(x\right), \tag{2.25}$$

subject to the boundary conditions:

$$\frac{dU}{dx}(a) = U_0 \text{ and } U(b) = U_N.$$

This problem is called a two point boundary value problem, since the boundary condition is given at two distinct points. To solve this equation by finite difference method, we will attempt to compute a gird function consisting of values

$$U_0,\ U_1,\ U_2,\ U_3, \cdots,\ U_N,$$

where U_i is our approximation to the solution U. Here, $x_i = x_0 + ih; \quad i = 1,\ 2,\ 3,\ \cdots,\ N$ and $h = \frac{b-a}{n}$. is the mesh width or the distance between grid points. The nodes are

$$a = x_1,\ x_2,\ x_3,\ \ \cdots,\ x_N = b$$

. At any node the equation (2.25) becomes

$$\frac{d^2U(x_n)}{dx^2} + A(x_n)\frac{dU(x_n)}{dx} + B(x_n)U(x_n) = D(x_n). \tag{2.26}$$

Assume, $U(x_i) = U_i,\ A(x_i) = A_i,\ B(x_i) = B_i$ and $D(x_i) = D_i$.
If we replace $\frac{d^2U(x_n)}{dx^2}$ and $\frac{dU(x_n)}{dx}$ by the centered difference approximations such as [29]

$$\frac{d^2U(x_n)}{dx^2} = \frac{U_{n+1} - 2U_n + U_{n-1}}{h^2} \tag{2.27}$$

and

$$\frac{dU(x_n)}{dx} = \frac{U_{n+1} - U_{n-1}}{2h} \tag{2.28}$$

we obtain the set of Eqs. (2.27) and (2.28) in Eq. (2.26),

$$\frac{U_{n+1} - 2U_n + U_{n-1}}{h^2} + A_n\frac{U_{n+1} - U_{n-1}}{2h} + B_nU_n = D_n \text{ for } n = 1,\ 2,\ 3, \cdots,\ N. \tag{2.29}$$

$$(2 - hA_n)U_{n-1} + \left(2h^2B_n - 4\right)U_n + (2 + hA_n)U_{n+1} = 2h^2D_n \text{ for } n = 1,\ 2,\ 3, \cdots,\ N. \tag{2.30}$$

Using notations

$$a_n = (2 - hA_n),\ b_n = \left(2h^2B_n - 4\right),\ c_n = (2 + hA_n)\ \textit{and}\ \gamma_n = 2h^2D_n, \tag{2.31}$$

$$a_nU_{n-1} + b_nU_n + c_nU_{n+1} = \gamma_n. \tag{2.32}$$

From the boundary conditions, $\frac{U_1 - U_0}{h} = U_n,\ U_N = b.$
We have, $U_0 = U_1 - U_nh,\ \mathrm{U}_N = b.$
In Eq (2.32), putting $r = 1,\ 2,\ 3, \cdots,\ N-1$,we obtain

$$
\begin{gathered}
\left(a_1+b_1\right)U_1+c_2U_2=a_1hU_0,\\
a_2U_1+b_2U_2+c_2U_3=\gamma_2,\\
a_3U_2+b_3U_3+c_3U_3=\gamma_3,\\
\vdots \qquad\qquad \vdots \qquad\qquad \vdots\\
a_{N-2}U_{N-3}+b_{N-2}U_{N-2}+c_{N-2}U_{N-1}=\gamma_{N-2},\\
a_{N-2}U_{N-3}+b_{N-1}U_{N-1}+c_{N-1}U_N=\gamma_{N-1}.
\end{gathered}
$$

We have a linear system of $(N-1)$ Eqs. For $(N-1)$ unknowns which can be written in the form

$$MY=S$$

where,

$$
M=\begin{bmatrix}
a_1+b_1 & c_1 & c_2 & \cdots & 0 & 0\\
0 & a_2 & b_2 & \cdots & 0 & 0\\
0 & 0 & a_3 & \cdots & 0 & 0\\
\vdots & \vdots & \vdots & \cdots & \vdots & \vdots\\
0 & 0 & 0 & \cdots & b_{N-2} & c_{N-2}\\
0 & 0 & 0 & \cdots & a_{N-1} & b_{N-1}
\end{bmatrix},
$$

$$
Y=\begin{bmatrix}
U_0\\ U_1\\ U_2\\ \vdots\\ U_{N-2}\\ U_{N-1}
\end{bmatrix},
$$

$$
S=\begin{bmatrix}
\gamma_1+ahU_a\\ \gamma_2\\ \gamma_3\\ \vdots\\ \gamma_{N-1}\\ \gamma_{N-1}-C_{N-1}U_b
\end{bmatrix}.
$$

Chapter 3

Ferromagnetic effects for peristaltic flow of Cu-blood nanofluid for different shapes of nanosized particles

3.1 Introduction

In this article, we consider Cu-blood nanofluid with effect of diverse shaped nanoparticles. For the efficient thermal conductivity of the nanofluids, the Hamilton-Crosser model is applied. In addition, through the lumen, heat transfer is also studied in this chapter. Analytical solutions are gained from momentum and energy equations with long wavelength and low Reynold number approximation technique, and the behavior of parameters of interest is elaborated graphically.

3.2 Formulation of the problem

Consider the flow of copper nanofluid of different geometries such as bricks, platelets and cylinders in the axisymmetric circular straight tube of finite length (L). The motion of the flow of different nanoparticles is controlled and managed by the external magnetic field. The outermost surfaces or walls of the artery or tubes exhibit peristaltic motion. The heat transfer analysis with different geometries of nanoparticles in the base fluid (blood) is considered. Moreover, a constant temperature T_0 has been taken at the sinusoidally propagating wall of the straight tube (Fig. 3.1).

The flow in the fixed tube is time dependent in the fixed coordinates system. The nanofluid flow is time independent in a wave frame coordinates system with the same speed as well as the wave moves in the Z-direction. The walls of the artery are considered as:

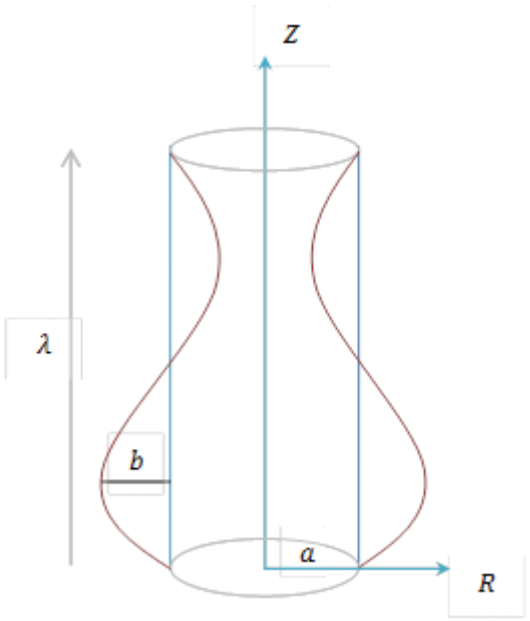

FIGURE 3.1: Schematic diagram of the artery.

.

$$\bar{R} = \bar{a} + \bar{b}sin(\tfrac{2\pi}{\lambda}(\bar{Z} - c\bar{t})), \text{ Upper wall}$$

$$-\bar{R} = -\bar{a} - \bar{b}sin(\frac{2\pi}{\lambda}(\bar{Z} - c\bar{t})), Lowerwall \tag{3.1}$$

In Eq. (3.1) c is the speed and λ denotes the wavelength.

3.3 Mathematical model

We consider the following definition of velocity

$$\bar{V} = [\bar{V}_{\bar{R}}(\bar{Z}, \bar{R}, \bar{t}), 0, \bar{V}_{\bar{Z}}(\bar{Z}, \bar{R}, \bar{t})] \tag{3.2}$$

The equations of the conservation of mass and the linear momentum of the unsteady flow of a nanofluid using a continuum approach

$$div\mathbf{V} = 0, \tag{3.3}$$

$$\rho_{nf}\frac{D\mathbf{V}}{Dt} = div\mathbf{S} + g(\rho\gamma)_{nf}(T - T_1) \tag{3.4}$$

$$(\rho c_p)_{nf}\frac{DT}{Dt} = \mathbf{S}\cdot\mathbf{L} + K_{nf}\nabla^2 T \tag{3.5}$$

Expression of Cauchy stress S tensor for viscous fluid is

$$\mathbf{S} = -p\mathbf{I} + \mu_{nf}\mathbf{A} \tag{3.6}$$

In which I is the identity tensor, $\bar{P}(\bar{Z},\bar{R},\bar{t})$ the pressure, μ_{nf} is the dynamic viscosity of nanofluid and the Rivlin- Erickson tensor A is

$$\mathbf{A} = \mathbf{L} + \mathbf{L}^T, \tag{3.7}$$

$$\mathbf{L} = grad\mathbf{V}, \tag{3.8}$$

Where superscript T represents the matrix transpose and

$$\mathbf{L} = \begin{bmatrix} \frac{\partial \bar{V}_r}{\partial \bar{R}} & \frac{1}{\bar{R}}\frac{\partial \bar{V}_r}{\partial \bar{\Theta}} - \frac{\bar{V}_\theta}{\bar{R}} & \frac{\partial \bar{V}_r}{\partial \bar{Z}} \\ \frac{\partial \bar{V}_{\Theta 3}}{\partial \bar{R}} & \frac{1}{\bar{R}}\frac{\partial \bar{V}_\Theta}{\partial \bar{\Theta}} + \frac{\bar{V}_r}{\bar{R}} & \frac{\partial \bar{V}_\Theta}{\partial \bar{Z}} \\ \frac{\partial \bar{V}_z}{\partial \bar{R}} & \frac{1}{\bar{R}}\frac{\partial \bar{V}_z}{\partial \bar{\Theta}} & \frac{\partial \bar{V}_z}{\partial \bar{Z}} \end{bmatrix}$$

$$\mathbf{L} = \begin{bmatrix} \frac{\partial \bar{V}_r}{\partial \bar{R}} & 0 & \frac{\partial \bar{V}_r}{\partial \bar{Z}} \\ 0 & \frac{\bar{V}_r}{\bar{R}} & 0 \\ \frac{\partial \bar{V}_z}{\partial \bar{R}} & 0 & \frac{\partial \bar{V}_z}{\partial \bar{Z}} \end{bmatrix}$$

$$\mathbf{L}^T = \begin{bmatrix} \frac{\partial \bar{V}_r}{\partial \bar{R}} & 0 & \frac{\partial \bar{V}_z}{\partial \bar{R}} \\ 0 & \frac{\bar{V}_r}{\bar{R}} & 0 \\ \frac{\partial \bar{V}_r}{\partial \bar{Z}} & 0 & \frac{\partial \bar{V}_z}{\partial \bar{Z}} \end{bmatrix}$$

Eq. (3.7) is of the form

$$\mathbf{A} = \begin{bmatrix} 2\frac{\partial \bar{V}_r}{\partial \bar{R}} & 0 & \frac{\partial \bar{V}_r}{\partial \bar{Z}} + \frac{\partial \bar{V}_z}{\partial \bar{R}} \\ \frac{\bar{V}_z}{\bar{R}} & 2\frac{\bar{V}_z}{\bar{R}} & 0 \\ \frac{\partial \bar{V}_r}{\partial \bar{Z}} + \frac{\partial \bar{V}_r}{\partial \bar{Z}} & 0 & 2\frac{\partial \bar{V}_z}{\partial \bar{Z}} \end{bmatrix}$$

The constitutive continuity equation, momentum and energy in the presence of body force for the considered geometry are

$$\frac{1}{\bar{R}}\frac{\partial \bar{V}_r}{\partial \bar{R}} + \frac{\partial \bar{V}_z}{\partial \bar{Z}} = 0, \tag{3.9}$$

$$\rho_{nf}(\bar{V}_r\frac{\partial\bar{V}_r}{\partial\bar{R}}+\bar{V}_z\frac{\partial\bar{V}_r}{\partial\bar{Z}})$$
$$=-\frac{\partial\bar{P}}{\partial\bar{R}}+\mu_{nf}\frac{\partial}{\partial\bar{R}}(2\frac{\partial\bar{V}_r}{\partial\bar{R}})+\mu_{nf}\frac{2}{\bar{R}}(\frac{\partial\bar{V}_r}{\partial\bar{R}}-\frac{\bar{V}_r}{\bar{R}})+\mu_{nf}\frac{\partial}{\partial\bar{Z}}(\frac{\partial\bar{V}_r}{\partial\bar{R}}+\frac{\partial\bar{V}_z}{\partial\bar{Z}}), \tag{3.10}$$

$$\rho_{nf}(\bar{V}_r\frac{\partial\bar{V}_z}{\partial\bar{R}}+\bar{V}_z\frac{\partial\bar{V}_z}{\partial\bar{Z}})$$
$$=-\frac{\partial\bar{P}}{\partial\bar{Z}}+\mu_{nf}\frac{\partial}{\partial\bar{Z}}(2\frac{\partial\bar{V}_z}{\partial\bar{Z}})+\mu_{nf}\frac{1}{\bar{R}}\frac{\partial\bar{V}_z}{\partial\bar{R}}(\bar{R}\frac{\partial\bar{V}_r}{\partial\bar{Z}}+\bar{R}\frac{\partial\bar{V}_z}{\partial\bar{R}})-\sigma B_0^2\bar{V}_z+\rho_{nf}g\alpha(\bar{T}-T_0), \tag{3.11}$$

$$(\rho_{cp})_{nf}(\bar{V}_r\frac{\partial T}{\partial\bar{R}}+\bar{V}_z\frac{\partial T}{\partial\bar{Z}})=k_{nf}(\frac{\partial^2T}{\partial\bar{R}^2}+\frac{1}{\bar{R}}\frac{\partial^2T}{\partial\bar{R}^2}+\frac{\partial^2T}{\partial\bar{Z}^2}). \tag{3.12}$$

Consider the flow of copper nanofluid of different geometries such as bricks, platelets and cylinders in the axisymmetric circular curved artery of finite length (L). The motion of the flow of different nanoparticles is controlled and managed by the external magnetic field. The outermost surfaces or walls of the artery or tubes exhibit peristaltic motion. The heat transfer analysis with different geometries of nanoparticles in the base fluid (blood) is considered. Moreover, a constant temperature T_0 has been taken at the sinusoidally propagating wall of the curved tube (Fig. 3.1).

The flow in the fixed tube is time dependent in the fixed coordinates system. The nanofluid flow is time independent in a wave frame coordinates system with the same speed as well as the wave moves in the Z-direction.

using the following transformations in the two frames are:

$$\bar{z}=\bar{Z}-c\bar{t},\quad \bar{r}=\bar{R},\quad \bar{v}_r=\bar{V}_r,\bar{v}_z=\bar{V}_z-c,\bar{p}(\bar{z},\bar{r},\bar{t})=\bar{P}(\bar{Z},\bar{R},\bar{t}). \tag{3.13}$$

The governing equations of motions representing an incompressible nanofluid can be expressed as:

$$\frac{1}{\bar{r}}\frac{\partial\bar{r}\bar{v}_r}{\partial\bar{r}}+\frac{\partial(\bar{v}_z+c)}{\partial(\bar{z}+c\bar{t})}=0, \tag{3.14}$$

$$\rho_{nf}(\bar{v}_r\frac{\partial\bar{v}_r}{\partial\bar{r}}+(\bar{v}_z+c)\frac{\partial\bar{v}_r}{\partial\bar{z}})$$
$$=-\frac{\partial\bar{p}}{\partial\bar{r}}+\mu_{nf}\frac{\partial}{\partial\bar{r}}(2\frac{\partial\bar{v}_r}{\partial\bar{r}})+\mu_{nf}\frac{2}{\bar{r}}(\frac{\partial\bar{v}_r}{\partial\bar{r}}-\frac{\bar{v}_r}{\bar{r}})+\mu_{nf}\frac{\partial}{\partial\bar{z}}(\frac{\partial\bar{v}_r}{\partial\bar{r}}+\frac{\partial(\bar{v}_z+c)}{\partial(\bar{z}+c\bar{t})}), \tag{3.15}$$

$$\rho_{nf}(\bar{v}_r\frac{\partial(\bar{v}_z+c)}{\partial\bar{r}}+(\bar{v}_z+c)\frac{\partial(\bar{v}_z+c)}{\partial(\bar{z}+c\bar{t})})$$
$$=-\frac{\partial\bar{p}}{\partial(\bar{z}+c\bar{t})}+\mu_{nf}\frac{\partial}{\partial(\bar{z}+c\bar{t})}(2\frac{\partial(\bar{v}_z+c)}{\partial(\bar{z}+c\bar{t})})+\mu_{nf}\frac{1}{\bar{r}}\frac{\partial(\bar{v}_z+c)}{\partial\bar{r}}(\bar{r}\frac{\partial\bar{v}_r}{\partial(\bar{z}+c\bar{t})}+\bar{r}\frac{\partial(\bar{v}_z+c)}{\partial\bar{r}}),$$
$$-\sigma B_0^2(\bar{v}_z+c)+\rho_{nf}g\alpha(\bar{T}-T_0) \tag{3.16}$$

$$(\rho_{cp})_{nf}(\bar{v}_r\frac{\partial T}{\partial\bar{r}}+\bar{v}_z\frac{\partial T}{\partial(\bar{z}+c\bar{t})})=k_{nf}(\frac{\partial^2T}{\partial\bar{r}^2}+\frac{1}{\bar{r}}\frac{\partial^2T}{\partial\bar{r}^2}+\frac{\partial^2T}{\partial(\bar{z}+c\bar{t})^2})+Q_0. \tag{3.17}$$

Simplifying above equations, we obtain;

$$\frac{1}{\bar{r}}\frac{\partial\bar{r}\bar{v}_r}{\partial\bar{r}}+\frac{\partial\bar{v}_z}{\partial\bar{z}}=0, \tag{3.18}$$

$$\rho_{nf}(\bar{v}_r\frac{\partial\bar{v}_r}{\partial\bar{r}}+\bar{v}_z\frac{\partial\bar{v}_r}{\partial\bar{z}})$$

$$=-\frac{\partial\bar{p}}{\partial\bar{r}}+\mu_{nf}\frac{\partial}{\partial\bar{r}}(2\frac{\partial\bar{v}_r}{\partial\bar{r}})+\mu_{nf}\frac{2}{\bar{r}}(\frac{\partial\bar{v}_r}{\partial\bar{r}}-\frac{\bar{v}_r}{\bar{r}})+\mu_{nf}\frac{\partial}{\partial\bar{z}}(\frac{\partial\bar{v}_r}{\partial\bar{r}}+\frac{\partial\bar{v}_r}{\partial\bar{z}}), \tag{3.19}$$

$$\rho_{nf}(\bar{v}_r\frac{\partial\bar{v}_z}{\partial\bar{r}}+\bar{v}_z\frac{\partial\bar{v}_z}{\partial\bar{z}})$$
$$=-\frac{\partial\bar{p}}{\partial\bar{z}}+\mu_{nf}\frac{\partial}{\partial\bar{z}}(2\frac{\partial\bar{v}_z}{\partial\bar{z}})+\mu_{nf}\frac{1}{\bar{r}}\frac{\partial\bar{v}_z}{\partial\bar{r}}(\bar{r}\frac{\partial\bar{v}_r}{\partial\bar{z}}+\bar{r}\frac{\partial\bar{v}_z}{\partial\bar{r}})-\sigma B_0^2(\bar{v}_z+c)+\rho_{nf}g\alpha(\bar{T}-T_0), \tag{3.20}$$

$$(\rho_{cp})_{nf}(\bar{v}_r\frac{\partial T}{\partial\bar{r}}+\bar{v}_z\frac{\partial T}{\partial\bar{z}})=k_{nf}(\frac{\partial^2T}{\partial\bar{r}^2}+\frac{1}{\bar{r}}\frac{\partial^2T}{\partial\bar{r}^2}+\frac{\partial^2T}{\partial\bar{z}^2})+Q_0. \tag{3.21}$$

where v_r and v_z are the velocities in the directions of axial and radial directions of the flow respectively. The fluid local temperature is T . Moreover, the effective

density is ρ_{nf}, the effective thermal conductivity is k_{nf},the effective thermal diffusibility is α_{nf},the effective dynamic viscosity is μ_{nf} and the heat capacitance is $(\rho c_p)_{nf}$ of the nanfluid.
We utilize the thermophysical properties which are mentioned as [30- 32].
$\mu_{nf} = \frac{\mu_f}{(1-\phi)^{2..5}}$,

$\rho_{nf} = \phi\rho_s + (1-\phi)\rho_f, (\rho\gamma)_{nf} = \phi(\rho\gamma)_s, + (1-\phi)(\rho\gamma)_f$

$$(\rho c_p)_{nf} = \phi(\rho c_p)_s + (1-\phi)(\rho c_p)_f. \tag{3.22}$$

In the above expressions ρ_f is density, μ_f is viscosity, the heat capacitance and thermal conductivity of base fluid represent $(\rho c_p)_f$ and k_f respectively. ρ_s is density, γ_s is thermal expansion coefficient, $(\rho c_p)_s$ is heat capacitance, k_s is thermal conductivity of the materials constituting Cu-nanoparticles and ϕ is the solid nanoparticle of nanofluid. By introducing a shape factor, Maxwell [33] and other worker have developed Hamilton and Crosser model [34] in which geometries of irregular particle taken into account As stated by this model, when the nanoparticles thermal conductivity is 100 times enhanced than of the base fluid, the expression of thermal conductivity of different geometries of nanoparticles will be:

$$\frac{k_{nf}}{k_f} = \left(\frac{k_s + (m+1)k_f - (m+1)(k_f - k_s)\phi}{k_s + (m+1)k_f + (k_f - k_s)\phi}\right) \tag{3.23}$$

here, the thermal conductivities of the particle material and the base fluid are k_s and k_f. The shape factors of geometries of nanoparticles is m in HamiltonCrosser model. As stated by them, the values of geometrical shape factor of nanoparticle are stated in Table 3.1 and Table 3.2.

Physical properties	Fluid phase (blood).	Cu
$c_p(J/kgK)$	3594	385
$\rho(kg/m^3)$	1063	8933
$k(W/mK)$	0.492	400
$\gamma/K \times 10^{-5}$	0.18	1.67

TABLE 3.1: Theromophysical properties of copper nanoparticles.

Nanoparticles	shape factor number
Platelets	5.7
Cylinders	4.9
Bricks	3.7

TABLE 3.2: Nanoparticles type and shape factor number.

The dimensional boundary conditions are:

$$\frac{\partial v_z}{\partial r} = 0, \frac{\partial \theta}{\partial r} = 0 \ at \ r = 0, v_z = -1, \theta = 0 \ at \ r = R(z) = 1 + \varepsilon cos(2\pi z) \quad (3.24)$$

In order to achieve the simplified governing equations, we bring into use the following non-dimensional quantities;

$$r = \frac{\bar{r}}{a}, \quad z = \frac{\bar{z}}{\lambda}, \quad v_r = \frac{\lambda \bar{v}_r}{ac}, \quad v_z = \frac{\bar{v}_z}{c}, \quad t = \frac{c\bar{t}}{\lambda},$$
$$p = \frac{a^2 \bar{p}}{\lambda c \mu_f}, \quad G_r = \frac{\rho_{nf} a^2 g \alpha T_0}{c\mu_f}, \quad \xi = \frac{Q_0 a^2}{T_0 k_{nf}}, \quad \theta = \frac{T - T_0}{T_0}.$$

Making use of these non-dimensional quantities in equations (3.18)to(3.21)

$$\frac{1}{ar}\frac{\partial\left(ar\frac{acv_r}{\lambda}\right)}{\partial(ar)} + \frac{\partial(cv_z)}{\partial(\lambda z)} = 0, \quad (3.25)$$

$$\rho_{nf}\left(\frac{acv_r}{\lambda}\frac{\partial\left(\frac{acv_r}{\lambda}\right)}{\partial(ar)} + cv_z\frac{\partial\left(\frac{acv_r}{\lambda}\right)}{\partial(\lambda z)}\right)$$
$$= -\frac{\partial\left(\frac{c\lambda\mu_f}{a^2}p\right)}{\partial(ar)} + \mu_{nf}\frac{\partial}{\partial(ar)}\left(2\frac{\partial\left(\frac{acv_r}{\lambda}\right)}{\partial(ar)}\right) + \mu_{nf}\frac{2}{ar}\left(\frac{\partial\left(\frac{acv_r}{\lambda}\right)}{\partial(ar)} - \frac{\frac{acv_r}{\lambda}}{ar}\right)$$
$$+ \mu_{nf}\frac{\partial}{\partial(\lambda z)}\left(\frac{\partial\left(\frac{acv_r}{\lambda}\right)}{\partial(ar)} + \frac{\partial(cv_z)}{\partial(\lambda z)}\right) \quad (3.26)$$

$$\rho_{nf}\left(\frac{acv_r}{\lambda}\frac{\partial(cv_z)}{\partial(ar)} + cv_z\frac{\partial(cv_z)}{\partial(\lambda z)}\right)$$

$$= -\frac{\partial\left(\frac{c\lambda\mu_f}{a^2}p\right)}{\partial(\lambda z)} + \mu_{nf}\frac{\partial}{\partial(\lambda z)}\left(2\frac{\partial(cv_z)}{\partial(\lambda z)}\right) + \mu_{nf}\frac{1}{ar}\frac{\partial(cv_z)}{\partial(ar)}\left(ar\frac{\partial\left(\frac{acv_r}{\lambda}\right)}{\partial(\lambda z)} + ar\frac{\partial(cv_z)}{\partial(ar)}\right)$$

$$- \sigma B_0^2(cv_z + c) + \rho_{nf} g\alpha\theta T_0 \tag{3.27}$$

$$(\rho_{cp})_{nf}\left(\frac{acv_r}{\lambda}\frac{\partial(\theta T_0 + T_0)}{\partial(ar)} + cv_z\frac{\partial(\theta T_0 + T_0)}{\partial(\lambda z)}\right)$$
$$= k_{nf}\left(\frac{\partial^2(\theta T_0 + T_0)}{\partial ar^2} + \frac{1}{ar}\frac{\partial^2(\theta T_0 + T_0)}{\partial(ar)^2} + \frac{\partial^2(\theta T_0 + T_0)}{\partial(\lambda z)^2}\right) + Q_0. \tag{3.28}$$

By simplifying above equations, we have

$$\frac{\partial v_r}{\partial r} + \frac{\partial v_z}{\partial z} = 0, \tag{3.29}$$

$$R_e\delta^3\frac{\rho_{nf}}{\rho_f}\left(\frac{\partial v_r}{\partial r} + v_z\frac{\partial v_r}{\partial z}\right)$$
$$= -\frac{\partial p}{\partial r} + \frac{\mu_{nf}}{\mu_f}\delta^2\frac{\partial}{\partial r}\left(2\frac{\partial v_r}{\partial r}\right) + \frac{\mu_{nf}}{\mu_f}\delta^2\frac{2}{r}\left(\frac{\partial v_r}{\partial r} - \frac{v_r}{r}\right) + \frac{\mu_{nf}}{\mu_f}\delta^3\frac{\partial}{\partial z}\left(\frac{\partial v_r}{\partial r} + \frac{\partial v_z}{\partial z}\right) \tag{3.30}$$

$$R_e\delta\frac{\rho_{nf}}{\rho_f}\left(\frac{\partial v_z}{\partial r} + v_z\frac{\partial v_z}{\partial z}\right)$$
$$= -\frac{\partial p}{\partial z} + \frac{\mu_{nf}}{\mu_f}\delta^2\frac{\partial}{\partial z}\left(2\frac{\partial v_z}{\partial z}\right) + \frac{\mu_{nf}}{\mu_f}\frac{1}{r}\frac{\partial v_z}{\partial r}\left(\delta^2\frac{\partial v_r}{\partial z} + r\frac{\partial v_z}{\partial r}\right) - \frac{\sigma a^2 B_0^2}{\mu_f}(v_z + 1)$$
$$+ \frac{\rho_{nf} g a^2\alpha T_0}{c\mu_f}\theta \tag{3.31}$$

$$\frac{ac}{k_f}\delta(\rho_{cp})_{nf}\left(v_r\frac{\partial\theta}{\partial r} + v_z\frac{\partial\theta}{\partial z}\right) = \frac{k_{nf}}{k_f}\left(\frac{\partial^2\theta}{\partial r^2} + \frac{1}{r}\frac{\partial\theta}{\partial r} + \delta^2\frac{\partial^2\theta}{\partial z^2}\right) + \frac{a^2 Q_0}{T_0 k_f}. \tag{3.32}$$

Applying the assumptions of long wavelength and low Reynolds number . We obtain the dimensionless form of constituting equations $(3.30 - 3.32)$ after releasing the dashes;

$$\frac{\partial p}{\partial r} = 0, \tag{3.33}$$

$$\frac{\partial p}{\partial z} = (1-\phi)^{-2.5}\left(\frac{\partial^2 v_z}{\partial r^2} + \frac{1}{r}\frac{\partial v_z}{\partial r}\right) - (v_z + 1)M^2 + G_r\theta \tag{3.34}$$

$$\frac{\partial^2\theta}{\partial r^2} + \frac{1}{r}\frac{\partial\theta}{\partial r} + \left(\frac{k_s - (k_s - k_f)\phi + (1+m)k_f}{k_s + (1+m)(k_s - k_f)\phi + (1+m)k_f}\right)\xi = 0. \tag{3.35}$$

here the Hartmann number,Grashof number and heat absorption parameter are M,G_r and ξ are respectively. The dimensionless appropriate boundary conditions taken as:

$$\frac{\partial\theta}{\partial r}=0,\frac{\partial v_z}{\partial r}=0 \;\; at \;\; r=0,\theta=0,v_z=-1 \;\; at \;\; r=R(z)=1+\varepsilon cos(2\pi z). \tag{3.36}$$

3.4 Solutions development

Solving Eqs. (3.35)-(3.36) together with boundary conditions in Eq. (3.37),we obtain:

$$v_z(r,z)=\frac{1}{4M^4(1-\phi)^{2.5}}[\;\frac{4I_0rM\sqrt{(1-\phi)^{2.5}}\Big(\;G_r\frac{k_f}{k_{nf}}\xi+M^2\frac{dp}{dz}(1-\phi)^{2.5}\;\Big)}{I_0hM\sqrt{(1-\phi)^{2.5}}}]$$

$$-4M^2(1-\phi)^{2.5}[M^2+\frac{dp}{dz}]+G_r\frac{k_f}{k_{nf}}\xi[M^2(R^2-r^2)(1-\phi)^{2.5}-4] \tag{3.37}$$

$$\theta(r,z)=\frac{1}{4}\left(\frac{k_s+(m+1)k_f+(k_f-k_s)\phi}{k_s+(m+1)k_f-(m+1)(k_f-k_s)\phi}\right)\xi(R^2-r^2) \tag{3.38}$$

In fixed frame the dimensional volume flow is defined as

$$\bar{Q}=\int_{-\bar{H}}^{\bar{H}}\bar{V}_z d\bar{R}, \tag{3.39}$$

In which $\bar{H}$ is a function of t and z. In wave frame above expression becomes

$$\bar{F}=\int_{-\bar{H}}^{\bar{H}}\bar{v}_z d\bar{r}, \tag{3.40}$$

where $\bar{H}$ is a function of z alone.

$$\bar{Q}=\bar{F}+2c\bar{H} \tag{3.41}$$

As a fixed position z, the time average flow over a period T is

$$\bar{Q}=\frac{1}{T}\int_0^{\bar{T}}Q dt. \tag{3.42}$$

Pluging Eq. (3.42) into Eq. (3.43) and then integrating, we get

$$\bar{Q} = \bar{q} + 2c\bar{a} \tag{3.43}$$

this implies:

$$\frac{dp}{dz} = \frac{1}{8M^4R^3I_2(1-\phi)^{2.5}}[I_0hM^2(1-\phi)^{2.5}[G_r\frac{k_f}{k_{nf}}\xi R^2(h^2M^2(1-\phi)^{2.5}-8)$$

$$-8M^2(F+R^2)(1-\phi)^{2.5}] + 16G_r\frac{k_f}{k_{nf}}\xi hI_1RM\sqrt{(1-\phi)^{2.5}}] \tag{3.44}$$

The expression $V_z = \frac{1}{r}\frac{\partial\psi}{\partial r}$ with $\psi = 0$ at $r = R(z) = 1 + \varepsilon cos(2\pi z)$. provides the corresponding stream function.
The pressure rise can be found by using the expression

$$\nabla P = \int_0^1 (\left(\frac{\partial P}{\partial z}\right))dz \tag{3.45}$$

3.5 Graphical results and discussion

The results obtained are analytical and discussed graphically for different physical parameter in the previous segment.Figure 3.2, shows the velocity distribution for various values of Hartmann parameter and also for geometrical shapes of the nanoparticles. It is seen that field of velocity rises proximate the outer wall of an artery or tube when Hartmann parameter M rises, but it falls in the middle of the tube. In addition, we noticed that the magnetic field is lower for bricks nanoparticle, the velocity is higher for cylinder nanoparticle, but when we enhance magnetic field than the velocity of Platelets particle also enhanced but for Bricks nanoparticle velocity field is lowered. Figure 3.3 depicts pressure rise against volume flow rate. It is analyzed that when Hartmann number M increased the pressure rise also increases and particularly, pressure rise for Platelets nanoparticles is higher as contrast to Bricks and Cylinder nanoparticles in the effective nanofluid conductivity for dissimilar forms of the geometries of nanoparticles.

On the temperature distribution, the effect of different forms of nanoparticles is shown In fig (3.6 and 3.7). The graphical analysis depicts that the temperature of the nanofluid within the tube is greater at the z=0 of the tube and notably smaller at the outer peristaltic walls of the tube. The temperature grows as we alter the geometrical shapes of

bricks nanoparticles to cylinders nanoparticles and then platelets nanoparticles, respectively. Furthermore, we noted that temperature field depressed when the heat absorption parameter increased ϵ. It is seen that thermal conductivity of the nanofluid increases if we include the particular brick shape nanoparticles in the base fluid. Figure 3.3 depicts the effect of different constraints on the pressure gradient. The pressure gradient shows sinusoidal charcterstics and it gets bigger with an increase in the Grashof number Gr, and its values dropped significantly as the Hartmann number M increases. Similar manners, the temperature rises, the pressure gradient is also enhances for platelets than that of cylinder and brick shaped nanoparticles shown in the figure 3.4 and3.5. The brick and cylinder shaped nanoparticles influenced on streamlines is shown in the figure(3.8-3.10). It is noted that the accumulation of bolus for Bricks nanoparticles are higher, but the expanse of the bolus of Bricks nanoparticle is smaller as compared to the Cylinder particles.

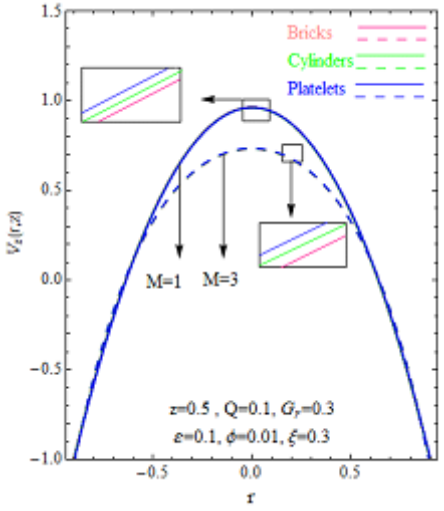

FIGURE 3.2: Influence of Hartman numbers M on velocity distribution.

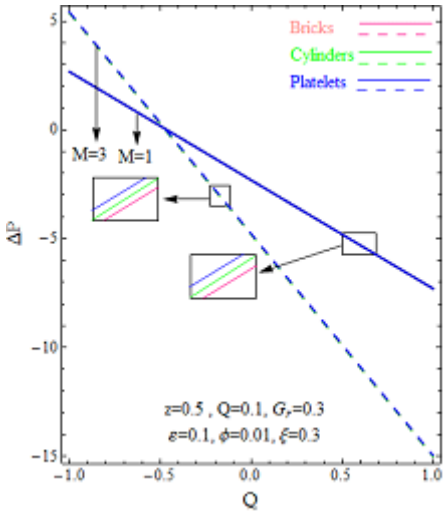

FIGURE 3.3: Influence of Hartman numbers M on pressure rise profile.

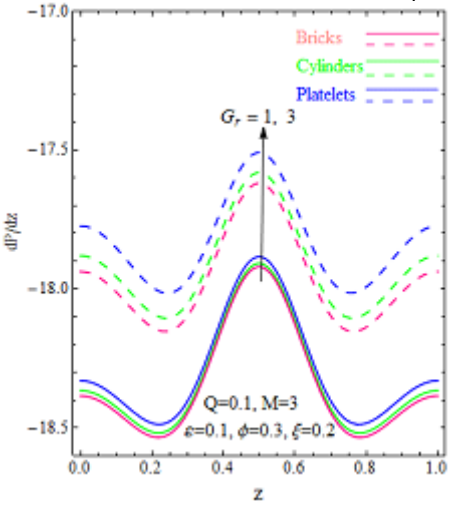

FIGURE 3.4: Influence of G_r on pressure gradient dp/dz .

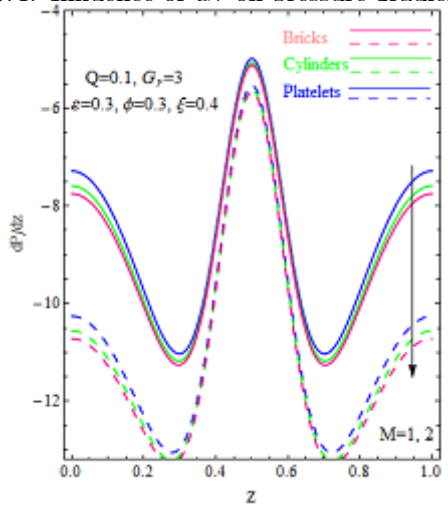

FIGURE 3.5: Influence of M on pressure gradient dp/dz.

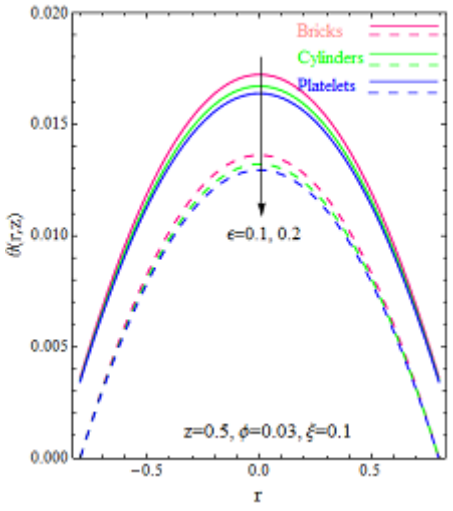

FIGURE 3.6: Influence of ε on temperature $\theta(r)$.

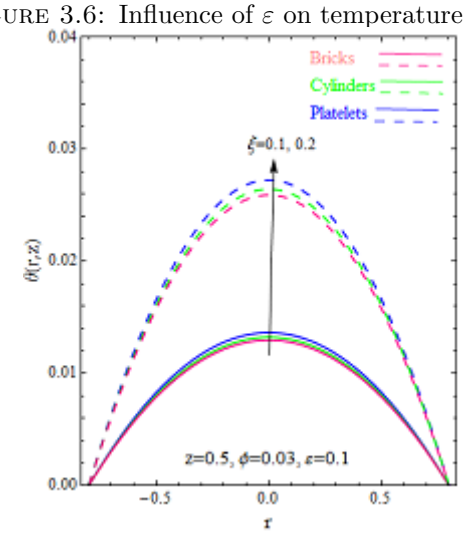

FIGURE 3.7: Influence of ξ on Temperature profile $\theta(r)$.

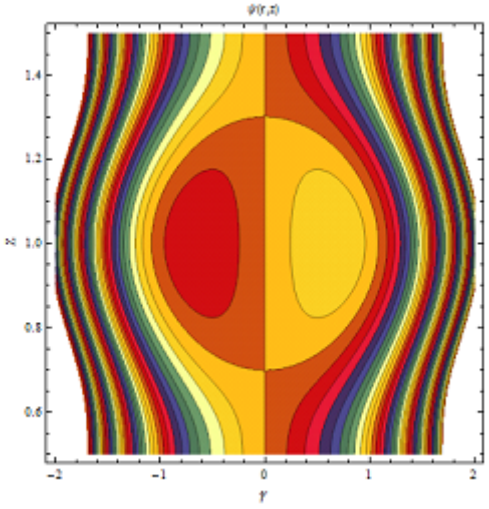

FIGURE 3.8: Contours for bricks

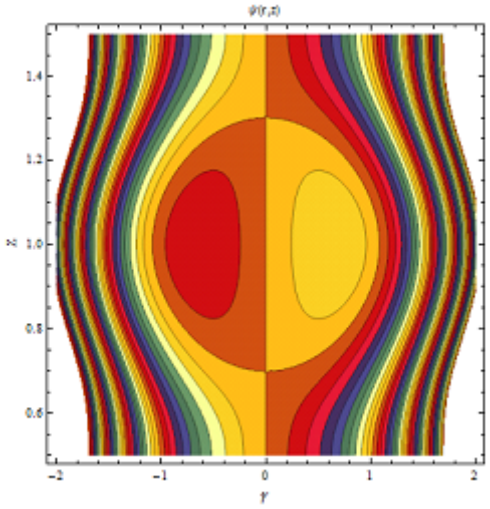

FIGURE 3.9: Contours for cylinders

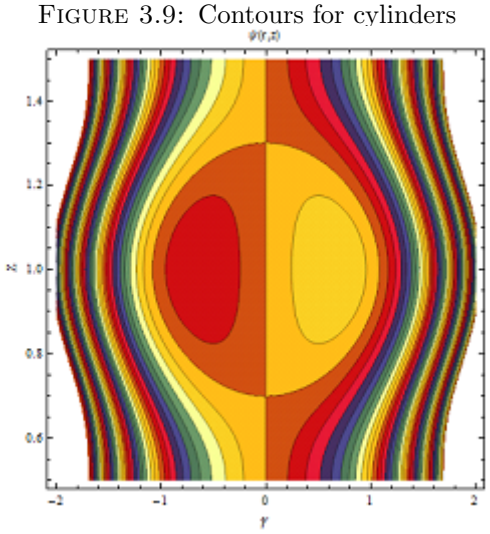

FIGURE 3.10: Contours for platelets.

3.6 Concluding remarks

In this study different geometry of nanoparticles such as bricks, cylinders and platelets mix with base fluid in straight channels under the effects of magnetic field. The behavior of all such particles is different in velocity profile, pressure rise, pressure gradient. The main findings are summarized as follows:

1. The velocity profile is depressing under the effects of increasing Hartmann number in the central axis of the tube where it slightly increases on outer propagating walls.

2. In the strong magnatic field effects bricks nanoparticles showing enhanced velocity profile than other nanoparticles.

3. Pressure rise developed as the Hartmann number increases and platelets nanoparticles remains higher than other sorts of nanoparticles.

4. The pressure gradient is clearly of sinusoidal form and it increases as the Grashof number increased.

5. The pressure gradient in the straight vertical artery is decreased as a heat source parameter increases.
   The temperature of all shapes of geometric nanoparticles is different, but source parameter in turn pressure gradient initiates to increase.

6. Stream lines exhibit that the flow in a vertical tube stays laminar under the effects of peristalsis in the variation of all the quantities available in this study.

Chapter 4

Numerical study of peristaltic flow of different shaped nanosize particles in curved channel with magnetic field effects

4.1 Introduction

In this chapter, we deal with the theoretical investigation of study of the peristaltic transport of nanofluids with effects of magnetic field. Three different geometries of nanoparticle namely bricks, cylinder and platelets are considered in our analysis. The flow geometry is considered as a curved artery to analyze the model for various biomedical applications. Numerical solutions are developed for the non-dimensional governing equations subject to physically pragmatic boundary conditions. The effects of nanoparticles shapes and the curvature of the artery on the axial velocity, for pressure rise, temperature, pressure gradient and streamlines in a curved channel with variation of different flow parameters are discussed with the help of graphical illustrations. It is observed that bricks shaped nanoparticles carry the maximum velocity at the middle of the artery, whereas far from the middle of the artery platelets nanoparticles exhibits maximum velocity. The study also inferred that the instantaneous flow characteristics are affected by the magnetic parameter and curvature parameter of the artery. It displays further that a magnetic field brings, the potential to control the flow of blood arteries, pressure rise and pressure gradient. It is also possible to bring down these parameters to any appropriate level by increasing/decreasing the degree of intensity of the

magnetic field. Thus, this study throws adequate light towards the therapeutic purpose of external magnetic field in the clinical and medical care of hemodynamic diseases.

4.2 Formulation of the problem

Consider the flow of copper nanofluid of different geometries such as bricks, platelets and cylinders in the axisymmetric circular curved artery of finite length (L). The motion of the flow of different nanoparticles is controlled and managed by the external magnetic field. The outermost surfaces or walls of the artery or tubes exhibit peristaltic motion. The heat transfer analysis with different geometries of nanoparticles in the base fluid (blood) is considered. Moreover, a constant temperature T_0 has been taken at the sinusoidally propagating wall of the curved tube (Fig. 4.1).

The flow in the fixed tube is time dependent in the fixed coordinates system. The nanofluid flow is time independent in a wave frame coordinates system with the same speed as well as the wave moves in the Z-direction. The walls of the artery are considered as: In the fixed coordinates $(\bar{R}, \bar{Z})$, the flow between the two tubes is unsteady. It

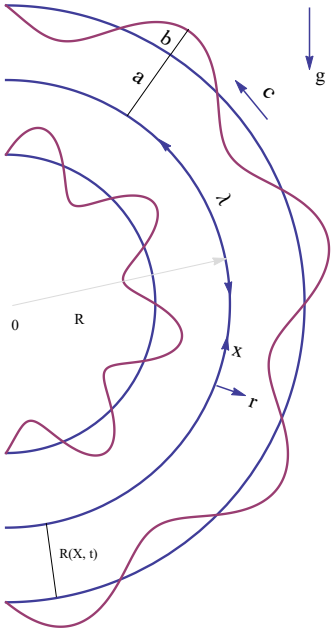

FIGURE 4.1: Schematic diagram of the curved artery.

becomes steady in a wave frame $(\bar{r}, \bar{z})$ moving with the same speed as the wave moves in the Z direction. The walls of the channel are considered as:

$$\bar{R} = \bar{a} + \bar{b}Sin\left(\frac{2\pi}{\lambda}(\bar{Z} - c\bar{t})\right), \quad \text{Upper wall} \tag{4.1}$$

$$-\bar{R} = -\bar{a} - \bar{b}Sin\left(\frac{2\pi}{\lambda}(\bar{Z} - c\bar{t})\right), \quad \text{Lower wall} \tag{4.2}$$

where c is the speed and λ denotes the wavelength.

4.3 Mathematical model

We consider the following definition of velocity

$$\bar{V} = [\bar{V_R}(\bar{Z}, \bar{R}, \bar{t}), \bar{V_\Theta}(\bar{Z}, \bar{R}, \bar{t}), 0]. \tag{4.3}$$

The equations of the conservation of mass and the linear momentum of the unsteady flow of a nanofluid using a continuum approach

$$\nabla \cdot \mathbf{V} = 0. \tag{4.4}$$

$$\rho_{nf} \frac{D\mathbf{V}}{Dt} = \nabla \cdot \mathbf{S} + g(\rho\gamma)_{nf}(T - T_1), \tag{4.5}$$

$$(\rho C_p)_{nf} \frac{D\mathbf{T}}{Dt} = \mathbf{L} + K_{nf}\nabla^2\mathbf{T}, \tag{4.6}$$

Expression of chauchy stress S tensor for viscous fluid is

$$\mathbf{S} = -p\mathbf{I} + \mu_{nf}\mathbf{A}. \tag{4.7}$$

In which I is the identity tensor, $p(\bar{Z}, \bar{R}, \bar{t})$ the pressure, μ_{nf} is the dynamic viscosity of nanofluid and the Rivlin- Erickson tensor A is

$$\mathbf{A} = \mathbf{L} + \mathbf{L^T}, \tag{4.8}$$

where,

$$\mathbf{L} = grad\mathbf{V}, \tag{4.9}$$

where superscript T represents the matrix transpose and

$$\mathbf{L} = \begin{bmatrix} \frac{\partial V_r}{\partial \bar{R}} & \frac{\bar{R}^*}{\bar{R}+\bar{R}^*}\frac{\partial V_r}{\partial \bar{z}} - \frac{\bar{V}_z}{\bar{R}+\bar{R}^*} & 0 \\ \frac{\partial V_z}{\partial \bar{R}} & \frac{\bar{R}^*}{\bar{R}+\bar{R}^*}\frac{\partial V_z}{\partial \bar{z}} + \frac{\bar{V}_r}{\bar{R}+\bar{R}^*} & 0 \\ 0 & 0 & 0 \end{bmatrix}$$

$$\mathbf{L}^T = \begin{bmatrix} \frac{\partial V_r}{\partial \bar{R}} & \frac{\partial V_z}{\partial \bar{R}} & 0 \\ \frac{\bar{R}^*}{\bar{R}+\bar{R}^*}\frac{\partial V_r}{\partial \bar{z}} - \frac{\bar{V}_z}{\bar{R}+\bar{R}^*} & \frac{\bar{R}^*}{\bar{R}+\bar{R}^*}\frac{\partial V_r}{\partial \bar{R}} - \frac{\bar{V}_z}{\bar{R}+\bar{R}^*} & 0 \\ 0 & 0 & 0 \end{bmatrix}$$

Eq. (4.8) is of the form

$$\mathbf{A} = \begin{bmatrix} 2\frac{\partial V_r}{\partial \bar{R}} & \frac{\bar{R}^*}{\bar{R}+\bar{R}^*}\frac{\partial V_r}{\partial \bar{z}} - \frac{\bar{V}_z}{\bar{R}+\bar{R}^*} + \frac{\partial V_z}{\partial \bar{R}} & 0 \\ \frac{\partial V_z}{\partial \bar{R}} + \frac{\bar{R}^*}{\bar{R}+\bar{R}^*}\frac{\partial V_r}{\partial \bar{z}} - \frac{\bar{V}_z}{\bar{R}+\bar{R}^*} & 2\left(\frac{\bar{R}^*}{\bar{R}+\bar{R}^*}\frac{\partial V_r}{\partial \bar{R}} - \frac{\bar{V}_z}{\bar{R}+\bar{R}^*}\right) & 0 \\ 0 & 0 & 0 \end{bmatrix}$$

The continuity, momentum and energy equations in the presence of body force for the considered geometry are

$$\frac{1}{\bar{R}}\frac{\partial(\bar{R}+\bar{R}^*)\bar{V}_r}{\partial \bar{R}} + R^*\frac{\partial \bar{V}_z}{\partial \bar{Z}} = 0, \tag{4.10}$$

$$\rho_{nf}\left(\bar{V}_r\frac{\partial \bar{V}_r}{\partial \bar{R}} + \frac{R^*\bar{V}_z}{\bar{R}+R^*}\frac{\partial \bar{V}_r}{\partial \bar{Z}} - \frac{\bar{V}_z^2}{\bar{R}+R^*}\right) = -\frac{\partial \bar{P}}{\partial \bar{R}}$$
$$+\mu_{nf}\left(\frac{1}{\bar{R}+R^*}\frac{\partial}{\partial \bar{R}}\left((\bar{R}+R^*)\frac{\partial \bar{V}_r}{\partial \bar{R}}\right) + \left(\frac{R^*}{\bar{R}+R^*}\right)^2\frac{\partial^2 \bar{V}_r}{\partial \bar{Z}^2} - \frac{\bar{V}_r}{(\bar{R}+R^*)^2} - \frac{2R^*}{\left(\bar{R}+R^*\right)^2}\frac{\partial \bar{V}_z}{\partial \bar{Z}}\right) \tag{4.11}$$

$$\rho_{nf}\left(\bar{V}_r\frac{\partial \bar{V}_z}{\partial \bar{R}} + \frac{R^*\bar{V}_z}{\bar{R}+R^*}\frac{\partial \bar{V}_z}{\partial \bar{Z}} + \frac{\bar{V}_r\bar{V}_z}{\bar{R}+R^*}\right) = -\frac{R^*}{\bar{R}+R^*}\frac{\partial \bar{P}}{\partial \bar{z}}$$
$$+\mu_{nf}\left(\frac{1}{\bar{R}+R^*}\frac{\partial}{\partial \bar{R}}((\bar{R}+R^*)\bar{V}_z) + \left(\frac{R^*}{\bar{R}+R^*}\right)^2\frac{\partial^2 \bar{V}_z}{\partial \bar{Z}^2} - \frac{\bar{V}_z}{(\bar{R}+R^*)^2} + \frac{2R^*}{(\bar{R}+R^*)^2}\frac{\partial \bar{V}_r}{\partial \bar{Z}}\right)$$
$$-\sigma B_0^2\bar{V}_z + \rho_{nf}g\alpha\left(\bar{T}-T_0\right) \tag{4.12}$$

$$(\rho c_p)_{nf}\left(\frac{\partial \bar{T}}{\partial \bar{R}} + \frac{R^*}{\bar{R}+R^*}\frac{\partial \bar{T}}{\partial \bar{Z}}\right) = k_{nf}\left(\frac{1}{\bar{R}+R^*}\frac{\partial \bar{T}}{\partial \bar{R}} + \frac{1}{\bar{R}}\frac{\partial^2 \bar{T}}{\partial \bar{R}^2} + \left(\frac{R^*}{\bar{R}+R^*}\right)\frac{\partial^2 \bar{T}}{\partial \bar{Z}^2}\right) + Q_0. \tag{4.13}$$

In the moving and fixed frames, the transformations are defined as::

$$\bar{r} = \bar{R}, \quad \bar{z} = \bar{Z} - c\bar{t}, \quad \bar{v_r} = \bar{V}_r, \qquad \bar{v_z} = \bar{V}_z - c, \qquad \bar{p}(\bar{z},\bar{r},\bar{t}) = \bar{P}(\bar{Z},\bar{R},\bar{t}) \tag{4.14}$$

The governing equations representing incompressible nanofluid expressed as:

$$\frac{1}{\bar{r}}\frac{\partial(\bar{r}\bar{v}_r)}{\partial \bar{r}} + \frac{\partial(\bar{v}_z+c)}{\partial \bar{z}} = 0, \tag{4.15}$$

$$\rho_{nf}\left(\overline{v}_r\frac{\partial \overline{v}_r}{\partial \overline{r}} + \frac{R^*(\overline{v}_z+c)}{\overline{r}+R^*}\frac{\partial \overline{v}_r}{\partial \overline{z}} - \frac{(\overline{v}_z+c)^2}{\overline{r}+R^*}\right)$$
$$= -\frac{\partial \overline{P}}{\partial \overline{r}} + \mu_{nf}\left(\frac{1}{\overline{r}+R^*}\frac{\partial}{\partial \overline{r}}\left((\overline{r}+R^*)\frac{\partial \overline{v}_r}{\partial \overline{r}}\right) + \left(\frac{R^*}{\overline{r}+R^*}\right)^2\frac{\partial^2 \bar{v}_r}{\partial \bar{z}^2} - \frac{\overline{v}_r}{(\overline{r}+R^*)^2} - \frac{2R^*}{\overline{r}+R^*}\frac{\partial \overline{v}_z}{\partial \overline{z}}\right) \tag{4.16}$$

$$\rho_{nf}\left(\bar{v}_r\frac{\partial\bar{v}_z}{\partial\bar{r}}+\frac{R^*(\bar{v}_z+c)}{\bar{r}+R^*}\frac{\partial\bar{v}_z}{\partial\bar{z}}+\frac{(\bar{v}_z+c)\bar{v}_r}{\bar{r}+R^*}\right)=-\frac{R^*}{\bar{r}+R^*}\frac{\partial\bar{P}}{\partial\bar{z}}$$

$$+\mu_{nf}\left(\frac{1}{\bar{r}+R^*}\frac{\partial}{\partial\bar{r}}\left((\bar{r}+R^*)\frac{\partial\bar{v}_z}{\partial\bar{r}}\right)+\left(\frac{R^*}{\bar{r}+R^*}\right)^2\frac{\partial^2\bar{v}_z}{\partial\bar{z}^2}-\frac{(\bar{v}_z+c)}{(\bar{r}+R^*)^2}-\frac{2R^*}{(\bar{r}+R^*)^2}\frac{\partial\bar{v}_r}{\partial\bar{z}}\right)\quad,$$

$$-\sigma B_0^2(\bar{v_z}+c)+\rho_{nf}g\alpha\left(\bar{T}-T_0\right)\qquad(4.17)$$

$$(\rho c_p)_{nf}\left(\frac{\partial\bar{T}}{\partial\bar{r}}+\frac{R^*}{\bar{r}+R^*}\frac{\partial\bar{T}}{\partial\bar{z}}\right)=k_{nf}\left(\frac{1}{\bar{r}+R^*}\frac{\partial\bar{T}}{\partial\bar{r}}+\frac{\partial^2\bar{T}}{\partial\bar{r^2}}+\left(\frac{R^*}{\bar{r}+R^*}\right)^2\frac{\partial^2\bar{T}}{\partial\bar{z}^2}\right)+Q_0.\qquad(4.18)$$

By simplifyig above equations, we obtain

$$\frac{1}{\bar{r}}\frac{\partial(\bar{r}\bar{v}_r)}{\partial\bar{r}}+\frac{\partial(\bar{v}_z)}{\partial\bar{z}}=0,\qquad(4.19)$$

$$\rho_{nf}\left(\overline{v}_r\frac{\partial\overline{v}_r}{\partial\overline{r}}+\frac{R^*(\overline{v}_z+c)}{\overline{r}+R^*}\frac{\partial\overline{v}_r}{\partial\overline{z}}-\frac{(\overline{v}_z+c)^2}{\overline{r}+R^*}\right)$$
$$=-\frac{\partial\bar{P}}{\partial\bar{r}}+\mu_{nf}\left(\frac{1}{\bar{r}+R^*}\frac{\partial}{\partial\bar{r}}\left((\bar{r}+R^*)\frac{\partial\bar{v}_r}{\partial\bar{r}}\right)+\left(\frac{R^*}{\bar{r}+R^*}\right)^2\frac{\partial^2\bar{v}_r}{\partial\bar{z}^2}-\frac{\bar{v}_r}{(\bar{r}+R^*)^2}-\frac{2R^*}{\bar{r}+R^*}\frac{\partial\bar{v}_z}{\partial\bar{z}}\right),\qquad(4.20)$$

$$\rho_{nf}\left(\bar{v}_r\frac{\partial\bar{v}_z}{\partial\bar{r}}+\frac{R^*(\bar{v}_z+c)}{\bar{r}+R^*}\frac{\partial\bar{v}_z}{\partial\bar{z}}+\frac{(\bar{v}_z+c)\bar{v}_r}{\bar{r}+R^*}\right)=-\frac{R^*}{\bar{r}+R^*}\frac{\partial\bar{P}}{\partial\bar{z}}$$

$$+\mu_{nf}\left(\frac{1}{\bar{r}+R^*}\frac{\partial}{\partial\bar{r}}\left((\bar{r}+R^*)\frac{\partial\bar{v}_z}{\partial\bar{r}}\right)+\left(\frac{R^*}{\bar{r}+R^*}\right)^2\frac{\partial^2\bar{v}_z}{\partial\bar{z}^2}-\frac{(\bar{v}_r+c)}{(\bar{r}+R^*)^2}-\frac{2R^*}{\bar{r}+R^*}\frac{\partial\bar{v}_r}{\partial\bar{z}}\right)$$

$$-\sigma B_0^2(\bar{v_z}+c)+\rho_{nf}g\alpha\left(\bar{T}-T_0\right),\qquad(4.21)$$

$$(\rho c_p)_{nf}\left(\frac{\partial\bar{T}}{\partial\bar{r}}+\frac{R^*}{\bar{r}+R^*}\frac{\partial\bar{T}}{\partial\bar{z}}\right)=k_{nf}\left(\frac{1}{\bar{r}+R^*}\frac{\partial\bar{T}}{\partial\bar{r}}+\frac{\partial^2\bar{T}}{\partial\bar{r^2}}+\left(\frac{R^*}{\bar{r}+R^*}\right)^2\frac{\partial^2\bar{T}}{\partial\bar{z}^2}\right)+Q_0.\qquad(4.22)$$

where v_r and v_z are the components of velocity along axial and radial directions of the flow respectively. The fluid local temperature is T . Moreover, the effective density is ρ_{nf}, the effective thermal conductivity is k_{nf},the effective thermal diffusibility is α_{nf},the effective dynamic viscosity is μ_{nf} and the heat capacitance is $(\rho c_p)_{nf}$ of the nanfluid. We utilize the thermophysical properties are given as

$$\mu_{nf} = \frac{\mu_f}{(1-\phi)^2}, \quad \rho_{nf} = (1-\phi)\,\phi_f + \phi\rho_s, \quad \rho_{nf} = (1-\phi)\,\phi_f + \phi\rho_s,$$
$$\rho_{nf} = (1-\phi)\,\phi_f + \phi\rho_s. \tag{4.23}$$

In the above expressions ρ_f is density, μ_f is viscosity,the heat capacitance and thermal conductivity of base fluid represent $(\rho c_p)_f$ and k_f respectively. ρ_s is density, γ_s is thermal expansion coefficient, $(\rho c_p)_s$ is heat capacitance, k_s is thermal conductivity of the materials constituting Cu-nanoparticles and ϕ is the solid nanoparticle of nanofluid. By introducing a shape factor, Maxwell [33] and other worker have developed Hamilton and Crosser model [34] in which geometries of irregular particle taken into account. As stated by this model, when the thermal conductivity nanoparticles is 100 times enhanced that of the base fluid, the expression of thermal conductivity of different geometries of nanoparticles will be

$$\frac{K_{nf}}{K_f} = \frac{k_s - (m+1)(k_f - k_s)\phi + (m+1)k_f}{k_s + (k_f - k_s)\phi + (m+1)k_f} \tag{4.24}$$

where, the thermal conductivities of the particle material and the base fluid are k_s and k_f. The shape factors of geometries of nanoparticles is m in HamiltonCrosser model. As stated by them, the values of geometrical shape factor of nanoparticle are stated in table 4.1 and table 4.2.

Nanoparticles	shape factor number
Platelets	5.7
Cylinders	4.9
Bricks	3.7

TABLE 4.1: Nanoparticles shape factor

Physical properties	Fluid phase (blood).	Cu
$c_p(J/kgK)$	3594	385
$\rho(kg/m^3)$	1063	8933
$k(W/mK)$	0.492	400
$\gamma/K \times 10^{-5}$	0.18	1.67

TABLE 4.2: Theromophysical properties of copper nanoparticles.

The dimensional boundary conditions are:

$$\frac{\partial v_z}{\partial r} = 0, \frac{\partial \theta}{\partial r} = 0 \quad \text{at} \quad r = 0, v_z = 0, \theta = 0 \quad \text{at} \quad r = R(z) = 1 + \epsilon cos(2\pi z). \tag{4.25}$$

In order to achieve the simplified governing equations, we bring into use the following nondimensional quantities:

$$r=\frac{\bar{r}}{a}, \qquad z=\frac{\bar{z}}{\lambda}, \qquad v_r=\frac{\lambda\bar{v}_r}{ac}, \qquad v_z=\frac{\lambda\bar{v}_z}{ac}, \qquad t=\frac{c\bar{t}}{\lambda},$$
$$p=\frac{a^2\bar{p}}{\lambda c\mu_f}, \quad G_r=\frac{\rho_{nf}a^2g\alpha T_0}{c\mu_f}, \quad \xi=\frac{Q_0a^2}{T_0k_{nf}}, \quad \theta=\frac{T-T_0}{T_0}.$$

Making use of these variables in Eqs.(4.19) to (4.22) :

$$\frac{1}{ar}\frac{\partial(ar\frac{arv_r}{\lambda})}{\partial(ar)}+\frac{\partial(cv_z)}{\partial(\lambda z)}=0, \tag{4.27}$$

$$\rho_{nf}\left(\frac{acv_r}{\lambda}\frac{\partial(\frac{acv_r}{\lambda})}{\partial(ac)}+\frac{R^*(cv_z+c)}{R^*+ar}\frac{\partial(\frac{acv_r}{\lambda})}{\partial(\lambda z)}-\frac{(cv_z+c)^2}{R^*+ar}\right)$$
$$=-\frac{\partial(\frac{c\lambda\mu_f}{a^2}p)}{\partial(ar)}+\mu_{nf}\left(\frac{1}{R^*+ar}\frac{\partial}{\partial(ar)}\left((R^*+ar)\frac{\partial(\frac{acv_r}{\lambda})}{\partial(ar)}\right)+\left(\frac{R^*}{R^*+ar}\right)^2\frac{\partial^2(\frac{acv_r}{\lambda})}{\partial(\lambda^2z)}\right.$$
$$\left.-\frac{(\frac{acv_r}{\lambda})}{(R^*+ar)^2}-\frac{2R^*}{R^*+ar}\frac{\partial(cv_z)}{\partial(\lambda z)}\right), \tag{4.28}$$

$$\rho_{nf}\left(\frac{acv_r}{\lambda}\frac{v_z}{\partial(ar)}+\frac{R^*(cv_z+c)}{R^*+ar}\frac{\partial(cv_z)}{\partial(\lambda z)}+\frac{(cv_z+c)\frac{acv_r}{\lambda}}{R^*+ar}\right)$$
$$=-\frac{R^*}{R^*+ar}\frac{\partial(\frac{c\lambda\mu_f}{a^2}p)}{\partial(\lambda z)}+\mu_{nf}\left(\frac{1}{R^*+ar}\frac{\partial}{\partial(ar)}\left((R^*+ar)\frac{\partial(cv_z)}{\partial(ar)}\right)+\left(\frac{R^*}{R^*+ar}\right)^2\frac{\partial^2(cv_z)}{\partial(\lambda z^2)}\right.$$
$$\left.-\frac{(\bar{v}_r+c)}{(R^*+ar)^2}-\frac{2R^*}{R^*+ar}\frac{\partial(cv_r)}{\partial(\lambda z)}-\sigma B_0^2(cv_z+c)+\rho_{nf}g\alpha\theta T_0, \right. \tag{4.29}$$

$$(\rho c_p)_{nf}\left(\frac{\partial(\theta T_0+T_0)}{\partial ar}+\frac{R^*}{ar+R^*}\frac{\partial(\theta T_0+T_0)}{\partial\lambda z}\right)$$
$$=k_{nf}\left(\frac{1}{ar+R^*}\frac{\partial(\theta T_0+T_0)}{\partial ar}+\frac{\partial^2(\theta T_0+T_0)}{\partial ar^2}+\left(\frac{R^*}{ar+R^*}\right)^2\frac{\partial^2(\theta T_0+T_0)}{\partial\lambda z^2}\right)+Q_0. \tag{4.30}$$

After simplifying the above Eqs.

$$\frac{\partial v_r}{\partial r}+\frac{\partial v_z}{\partial z}=0, \tag{4.31}$$

$$R_e\delta^3\frac{\rho_{nf}}{\rho_f}\left(\frac{\partial v_r}{\partial r}+\frac{(v_z+1)}{r+k}\frac{\partial v_r}{\partial z}-\frac{(v_z+1)^2}{r+k}\right)=-\frac{\partial p}{\partial r}$$
$$+\mu_{nf}\left(\delta^2\frac{1}{r+k}\frac{\partial}{\partial r}\left((r+k)\frac{\partial v_r}{\partial r}\right)+\delta^2\left(\frac{1}{r+k}\right)^2\frac{\partial^2 v_r}{\partial z^2}-\delta^2\frac{v_r}{(r+k)^2}-2\delta^2\frac{1}{r+k}\frac{\partial v_z}{\partial z}\right), \tag{4.32}$$

$$R_e\left(V_r\frac{\partial V_z}{\partial r}+\delta\frac{k(V_z+1)}{k+r}\frac{\partial V_z}{\partial r}+\frac{V_z+1}{k+r}\right)=-\frac{k}{k+r}\frac{\partial p}{\partial z}$$
$$+\frac{\mu_{nf}}{\mu_f}\left(\frac{1}{k+r}\frac{\partial}{\partial r}\left((k+r)\frac{\partial V_z}{\partial r}\right)+\delta^2\left(\frac{k}{k+r}\right)^2\frac{\partial^2 V_z}{\partial z^2}+\frac{V_z+1}{(k+r)^2}-\delta\frac{2k}{(k+r)^2}\frac{\partial V_r}{\partial z}\right)$$
$$-\frac{a^2}{c\mu_f}(\rho\beta)_{nf}gT_0\theta-\frac{\sigma B_0^2a^2K}{\mu_f}(V_z+1) \tag{4.33}$$

$$R_e\delta\left(\rho c_p\right)_{nf}\left(\frac{\partial\theta}{\partial r}+\frac{k}{k+r}\frac{\partial\theta}{\partial z}\right)=\frac{k_{nf}}{k_f}\left(\frac{1}{k+r}\frac{\partial\theta}{\partial r}+\frac{\partial^2\theta}{\partial r^2}+\delta^2\left(\frac{k}{k+r}\right)^2\frac{\partial^2\theta}{\partial z^2}\right)+\frac{a^2Q_0}{T_0k_f}. \tag{4.34}$$

Considering the assumptions of low Reynolds number and larger wavelength. We obtain the dimensionless form of constituting equations (4.32)- (4.34).

$$\frac{\partial p}{\partial r}=0, \tag{4.35}$$

$$\frac{\partial p}{\partial z}=\frac{1}{(1-\phi)^2}\left(\frac{1}{k+r}\frac{\partial}{\partial r}\left((k+r)\frac{\partial v_z}{\partial r}\right)-\frac{v_z+1}{(k+r)^2}-\frac{2k}{(k+r)^2}\frac{\partial v_z}{\partial r}\right)$$
$$-M^2(v_z+1)+G_r\theta, \tag{4.36}$$

$$\frac{1}{r+k}\frac{\partial}{\partial r}\left((r+k)\frac{\partial\theta}{\partial r}\right)+\frac{k_s+(m+1)k_f-(m+1)(k_f-k_s)\phi}{k_s+(m+1)k_f+(k_f-k_s)\phi}\xi=0. \tag{4.37}$$

where, the heat absorption parameter, Hartmann number and Grashof number are respectively denoted as ξ, M and G_r.

The dimensionless boundary conditions are stated as:

$$\frac{\partial\theta}{\partial r}=0,\frac{\partial v_z}{\partial r}=0 \quad \text{at} \quad r=0,\theta=0,v_z=0 \quad \text{at} \quad r=R(z)=1+\epsilon cos(2\pi z). \tag{4.38}$$

4.4 Solutions development

The transformed governing equations (4.36) and (4.37) subject to the boundary conditions (4.38) are solved numerically utilizing the finite difference scheme. The central differences are employed to discritize the derivatives.

$$\frac{\partial^2 U(x_n)}{\partial x^2}=\frac{U_{n+1}-2U_n+U_{n-1}}{2h}, \tag{4.39}$$

and

$$\frac{\partial U(x_n)}{\partial x}=\frac{U_{n+1}-U_{n-1}}{h^2}, \tag{4.40}$$

we obtain the set of equations as

$$\frac{U_{n+1}-2U_n+U_{n-1}}{2h}+A_n\frac{U_{n+1}-U_{n-1}}{h^2}+B_nU_n=D_n \quad \text{for} \quad n=1,2,3,...,N \tag{4.41}$$

$$(2-hA_n)U_{n-1}+(2h^2B_n-4)U_n+(2+hA_n)U_{n+1}=2h^2D_n \quad \text{for} \quad n=1,2,3,...,N \tag{4.42}$$

Using notations

$$a_n=2-hA_n,$$

$$b_n=2h^2B_n-4,$$

$$c_n=2+hA_n,$$

and

$$\gamma_n=2h^2D_n.$$

$$a_nU_{n-1}+b_nU_n+c_nU_{n+1}=\gamma_n \tag{4.43}$$

From the boundary conditions

$$\frac{U_1-U_0}{h}=U_n, \quad U_N=b, \tag{4.44}$$

$$U_0=U_1-U_nh, \quad U_N=b. \tag{4.45}$$

4.5 Graphical results and discussion

The numerical solutions achieved by using the finite difference scheme in the previous section have been investigated graphically for various physical parameters. Figure 4.2 displays the velocity distribution for various geometrical shapes of the nanoparticles i.e., (Bricks, cylinders, Platelets) and unlike values of curvature parameter K of curved tube. It is shown that when we enhance curvature parameter K the field of velocity enhances near the center of the curved peristaltic tube rapidly than at the neighborhood of the wall. It is also depicted that velocity distribution is a little higher for nanoparticles of the bricks than that of the nanoparticles of cylinders and platelets with each values of curvature paramaeter K. This means that in straight arteries the Bricks, Cylinder and Platelets nanoparticles significantly enhance its velocity. Figure. 4.3 presents variant of velocity distribution for distinct geometries (shaped) of the nanoparticles with varying Hartmann parameter M. It is presented that when we enhance Hartmann parameter M velocity distribution decreases slightly near the tube wall as well as significantly at the center of the curved tube. It is depicted that by enhancing Hartmann parameter M velocity distribution depressed. Bricks particles showing higher velocity than the cylinder particle and platelet particles when exposing all of them in a magnetic field. Figure 4.4 presents changes occur in velocity distribution for various geometries of the nanoparticles with varying heat source parameter ξ. This velocity distribution depicts that when we enhance heat source parameter ξ the distribution of velocity decreases adjacent to the outer wall as well as at the central position of the curved tube. Figure 4.5 presents changes occur in velocity distribution for various geometries of the nanoparticles with varying Grashof number G_r. This velocity distribution depicts that when we enhance Grashouf number G_r the distribution of velocity increases adjacent to the outer wall as well as at the central position of the curved tube. Bricks geometries of nanoparticles improve the speed than the other shapes of nanoparticles in the velocity distribution.

Figures 4.6 and 4.7 are drawn for the important parameter of interest, Figuer 4.6 present pressure rise against flow rate. It is seen that when enhancing curvature parameter K pressure rise also enhanced for Bricks as compared Cylinder and Platelets nanoparticles geometries. It is also noted that for Platelets nanoparticles pressure decreases in the flow rate region ($-1 \leq F \leq 0$) but it shows reverse character in the region ($0 \leq F \leq 1$), similar behavior is maintained by other nanoparticles, Cylinder nanoparticles changes in the region ($-1 \leq F \leq 0.05$) and opposite behavior in the region ($0.05 \leq F \leq 1$) and Brickes nanoparticles changes in the region ($-1 \leq F \leq 0.1$) and opposite behavior in the region ($0.1 \leq F \leq 1$)). For positive values of flow rate the pressure rise increase as compared to negative values of flow rate. Figure 4.7 displays pressure rise against flow

rate. It is seen that when we enhance Hartmann parameter M pressure rise enhances for Bricks as compared other shaped geometries of nanoparticles. It is noticed that, for Platelets nanoparticles the pressure P decreases in the flow rate region ($-1 \leq F \leq 0.05$) but it shows reverse character in the region ($0.05 \leq F \leq 1$), similar behavior is maintained by other nanoparticles, Cylinder nanoparticles changes in the region ($-1 \leq F \leq 0.05$) and opposite behavior in the region ($0.05 \leq F \leq 1$) and Brickes nanoparticles changes in the region ($-1 \leq F \leq 0.1$) and opposite behavior in the region ($0.1 \leq F \leq 1$). For positive values of flow rate, the pressure rise increases as compared to negative values of flow rate.Now we discuss the effects of different parameters of interest on the pressure gradient of the problem in Figures 4.8 and 4.9. It is observed that the pressure gradient has a sinusoidal behavior and its increases with the increase in curvature parameter K and its values fall significantly as enhances the Hartmann parameter M. The pressure gradient is larger for platelets geometry nanoparticles than than that of the cylinder and brick sized nanoparticles for curvature parameter while it falls for the increase in Hartmann number. The impact of different shapes geometries of nanoparticles on the temperature profile is depicted in Figures. 4.10 and 4.11. The temperature of the nanofluid containing different nanoparticles within the tube is greater at the central section and depressed at the outer peristaltic walls. Temperature increases from bricks to cylinders and platelets geometrical nanoparticles, respectively. Further we observe that temperature profile depressed with the increase in the heat absorption parameter ξ and it also depressed when amplitude of the peristaltic wall ϵ increases. Trapping represents an interesting phenomenon for the fluid flow. This phenomenon gain more attracting in the presence of different geometrical shaped Cu-nanoparticles in peristalsis. Figure. (4.12-4.14) reveals that the size of the tapping bolus of Bricks nanoparticles is smaller than the boluses formation with cylinder and Platelets shaped nanoparticles. It is depicted that the number of bolus for Bricks particles are more than any other nanoparticles but size of the bolus formed by Bricks nanoparticle is compact as compare to the Cylinder nanoparticles and Platelets nanoparticles geometeries.

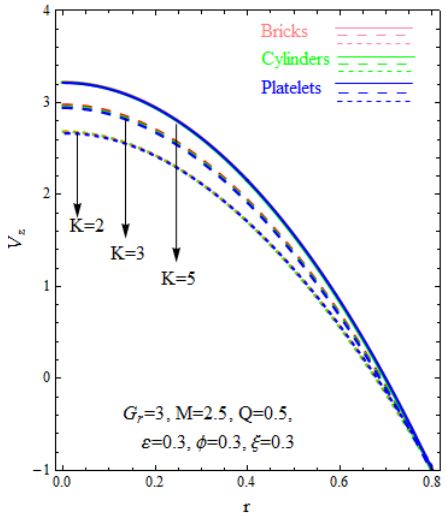

FIGURE 4.2: Influence of K on velocity profile for different shape of the nanoparticles.

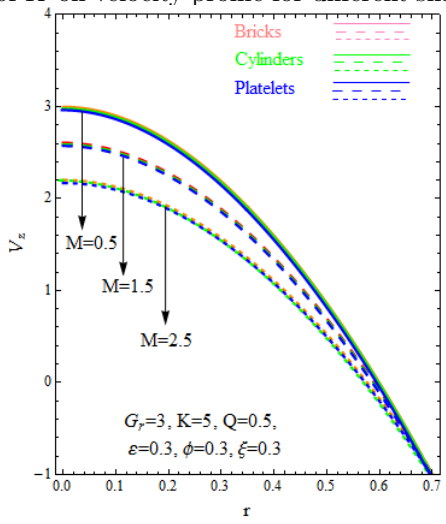

FIGURE 4.3: Influence of M on velocity profile for different shape of the nanoparticles.

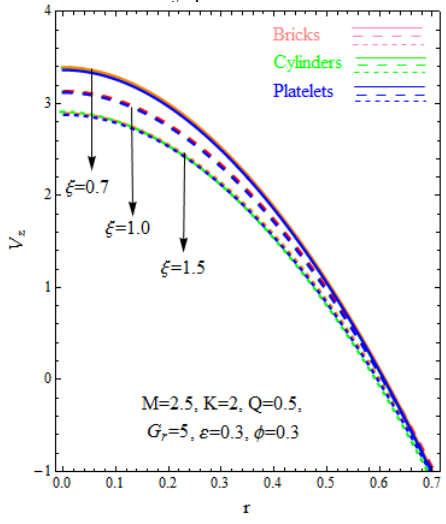

FIGURE 4.4: Influence of ξ on velocity profile for different shape of the nanoparticles.

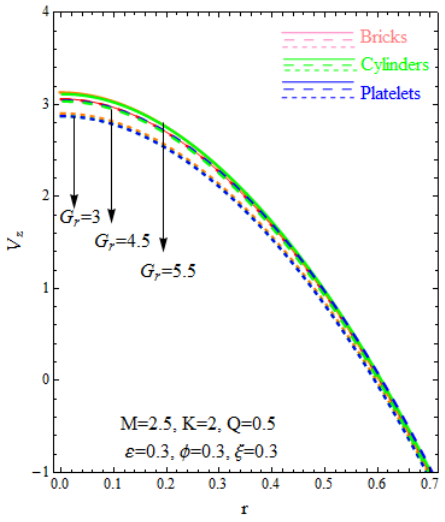

FIGURE 4.5: Influence of G_r on velocity profile for different shape of the nanoparticles.

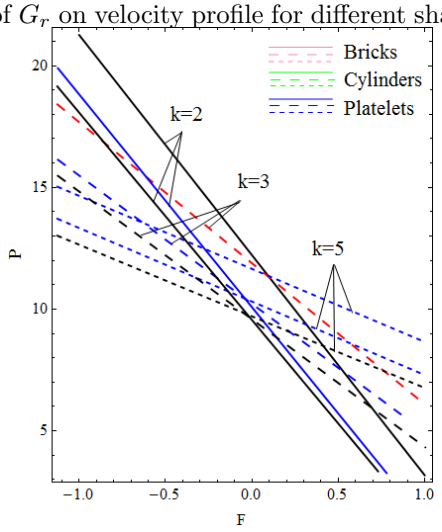

FIGURE 4.6: Influence of K on pressure rise for different shape of the nanoparticles.

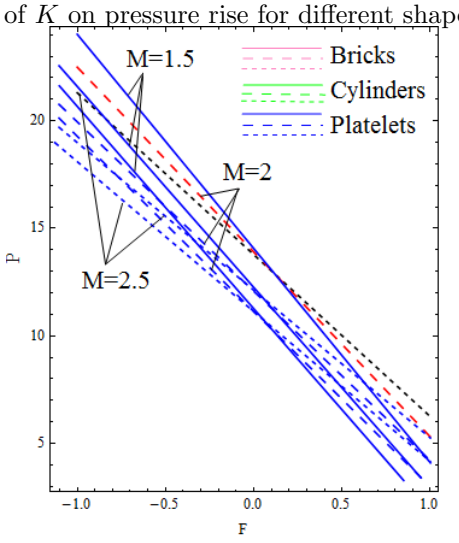

FIGURE 4.7: Influence of M on pressure rise for different shape of the nanoparticles.

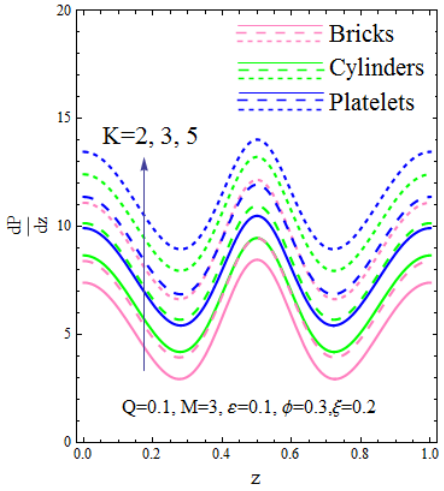

FIGURE 4.8: Influence of K on pressure gradient dp/dz.

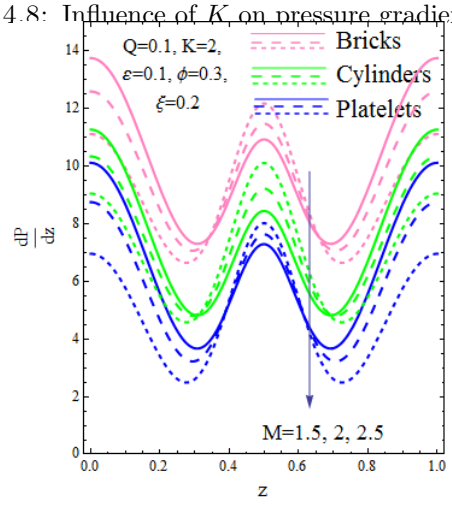

FIGURE 4.9: Influence of M on pressure gradient dp/dz.

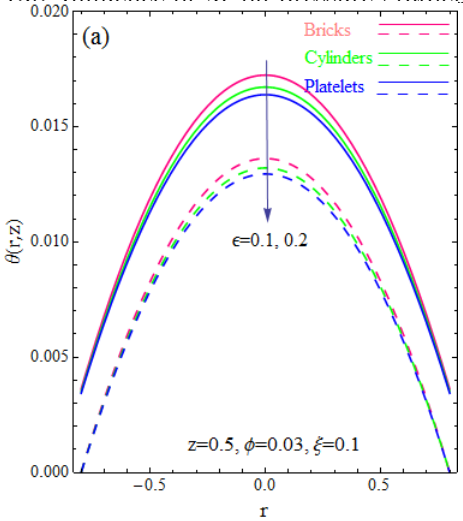

FIGURE 4.10: Influence of ϵ on temperature profile $\theta(r)$.

4.6 Concluding remarks

Numerical solutions are developed for the non-dimensional governing equations subject to physically pragmatic boundary conditions. The effects of nanoparticles shapes and

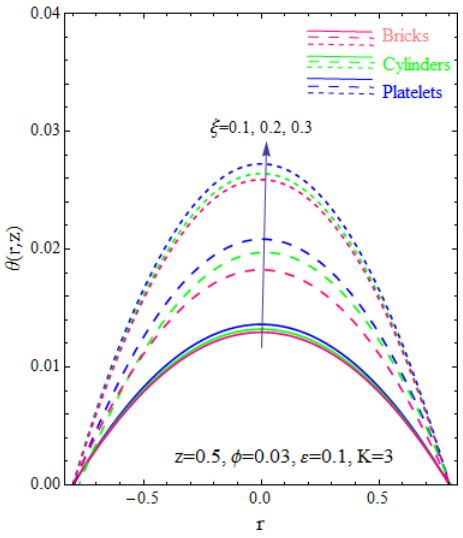

FIGURE 4.11: Influence of ξ on temperature profile $\theta(r)$.

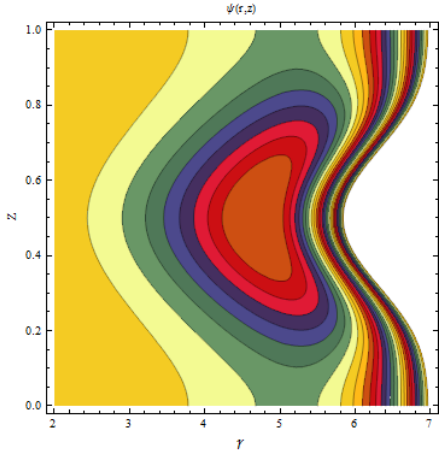

FIGURE 4.12: Contours for bricks.

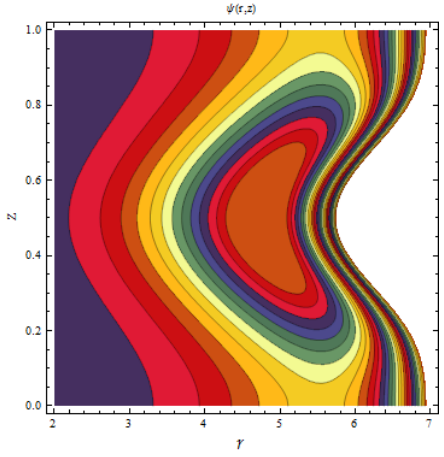

FIGURE 4.13: Contors for cylinders.

the curvature of the artery on the axial velocity, for pressure rise, temperature, pressure gradient and streamlines in a curved channel with variation of different flow parameters. The main findings are summarized as follows:

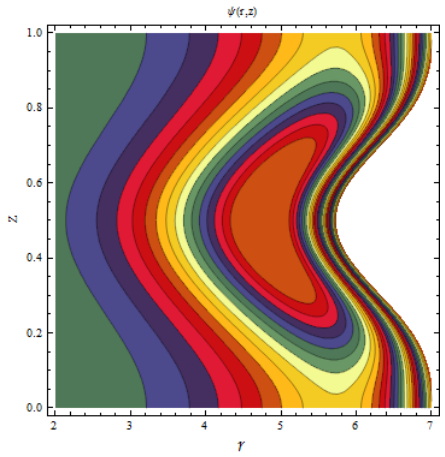

FIGURE 4.14: Contours for platelets.

r	Bricks	Cylindrs	Platelets
0	2.957017	2.956916	2.956869
0.1	2.866349	2.866258	2.866218
0.2	2.604559	2.604505	2.604480
0.3	2.184190	2.184188	2.184187
0.4	1.616697	1.616752	1.616778
0.5	0.896117	0.896212	0.896256
0.6	0.023503	0.023592	0.023634
0.7	-1	-1	-1

TABLE 4.3: Numerical values of velocity profile at Bricks, Cylindrs and Platelets for different nodes.

1. By enhancing curvature parameter K field of velocity enhances near the center of the curved peristaltic tube rapidly than at the neighborhood of the wall.

2. It is also depicted that velocity distribution is a little higher for nanoparticles of the bricks form than for nanoparticles of cylinders and platelets form with each value of curvature paramaeter K.

3. Hartmann parameter M then then velocity distribution decreases slightly near the tube wall as well as significantly at the centre curved tube. tube.

4. It is depicted that by enhancing Hartmann parameter M velocity distribution depressed. Bricks particles showing higher velocity than the cylinder particle and platelet particles when exposing all of them in a magnetic field.

5. The velocity distribution depicts that when we enhance source parameter ξ the distribution of velocity decreases adjacent to the outer wall as well as at the central position of the curved tube. Bricks geometries of nanoparticles improve the speed than the other shapes of nanoparticles in the velocity distribution.

6. By increasing Hartmann parameter M pressure rise enhances for Bricks as compared to other shaped geometries of nanoparticles.

7. Pressure gradient shows a sinusoidal characteristic and it increases with the increase in curvature parameter K and its values fall significantly as the enhances Hartmann parameter M.

8. By increasing Hartmann parameter M pressure rise enhances for Bricks as compared to other shaped geometries of nanoparticles. The pressure gradient holds larger values for platelets geometry nanoparticles than which of the briks and cylinder shaped nanoparticles for curvature parameter while it falls for the increase in Hartmann number.

9. Temperature profile is symmetric about central line.The temperature of the bricks nanoparticles falls down with the increase of heat source paramaqter ξ whereas temperature of cylinder and platelets nanoparticles enhance significantly.

10. The trapping bolus has smaller size for the Bricks nanoparticles as compaired to the boluses formation as compared to other shaped nanoparticles under our consideration.

11. The boluses for Bricks particles are greater in number than any other kind nanoparticles.

Chapter 5

Conclusion

In the present study, it is investigated that the effects and behaviour of different types of nanoparticles such as Bricks, cylinders and platelets in curved tube in the exposition and presence of magnetic field with symmetric boundary conditions in both momentum and energy equations. Numerical solution of these modelled ODEs are acquired by using Finite Difference method which is usefull to solve fluid mechanics problems for complicated geometries. Graphical results are provided to analyse the flow behaviour in the curved tube with peristaltic walls.

It is evident that blood flows carring oxygen and other vital nutrients through blood arterial system. At some positions in human body artries are straight, vertical, curved and bifurcated. So clearly flow of blood effects greatly by the physiology of arteries. Plenty of work regarding parastaltic flow is available in literature whereas very few research has been conducted in curved tubes /arteries. But the nanoparticles of different geometries immersed in blood flowing through curved tube. In curved tube curvature of tubes/arteries notably influences blood flows. It is seen in chapter four curvature of artery decreases blood flow in centre of the tube.For controlling and managing flows magnetic fields are imposed. As we have observed that Hartman number hinders the flow. Moreover by applying heat source parameter,flow of blood decreases where as Garshof number favors the flow. The curvature and magnetic field also effects the pressure of the system. We have seen in chapter four the curvature of artery increases pressure in the lower part of artery and decreases in the upper part of artery, the same results are drown with the magnetic field which is exposed externally to the human body.

Bibliography

[1] F.Yin,Y.C.Fung. Peristaltic waves in circular cylindrical tubes, Journal Applied Mechanics 36,(1969),579-587.

[2] J. C Burns,T. Parkes,Peristalatic motion, Journal of Fluid Mechanics 29,(1967), 731-743.

[3] L.M.Srivastava, V.PSrivastava,Peristaltic transport of a particle-Fluid suspension, Journal of Biomechanics and Engieering 111,(1989),157-1.

[4] N.A.S. Afifi, N.S. Gad, Interaction of peristaltic flow with pulsatile magneto-fluid through a porous medium, Acta Mechanica 149,(2001),229-237.

[5] J. C. Misra ,S.K.Pandey, Peristaltic transport of blood in small vessels: study of a mathematical model, Computers Mathematics with Applications 43,(2002), 1183-1193.

[6] Kh.S Mekheimer,Peristaltic flow of bleed under effect of a magnetic field in a nonuniform channels model,Applied Mathematics and Computation 153,(2004), 763-777.

[7] S. Nadeem,N.S Akbar, Effects of heat transfer on the peristaltic transport od MHD Newtonion fluid with variable viscosity:application of Adomian decomposition method,Communications in Nonlinear Science and NumericalSimulation 14,(2009), 3844-3855.

[8] M. V. Subba Reddy, M. Mishra, S.Sreenadh, A.R.Rao Influence of lateral walls on peristaltic flow in a rectangular duct ,Journal of Fluids Engineering 127,(2005), 824-827.

[9] V.Aranda, R.Cortez ,L. Fauci, Stokesian peristaltic pumping in a three-dimensional tube with a phase shifited asymmetric rectangular duct. Physics Fluids 23,(2011), 081901-081910.

[10] Kh.S.Mekhmeimer,S.Z.A. Husseny,A. I.Abd el Lateef ,effect of lateral walls on peristaltic flow through an asymmetric rectangular duct.Applied Bionics and Biomechanics 8,(2011),295-308.

[11] S. Akram, Kh.S. Mekhmeimer, S Nadeem, Influence of Lateral walls on peristaltic flow of a couple stress fluid in a non-uniform rectangular duct ,Applied Mathematics Information Science 8. (2014),11-27.

[12] T.W. Latham,Fluid motion in a peristaltic pump,Masschusetts Intitute of Technology, Cambridge, (1966).

[13] S.Srinivas, M. Kothandapani, IPeristaltic transport in an asymmetric channel with heat transfer, Heat and Mass transfer 35,(2008),514-514.

[14] KH. S. Mekheimer, Y.A. Elmaboud, Peristaltic flow through a porous medium in an annulus: application of an endoscope, Applied Mathematics Information Sciences 2, (2008),103-121

[15] C.Vasudev, U.R. Rao, G.P. Rao, M.V.SW. Reddy, Peristaltic Flow of a Newtonian fluid on Porous medium in a vertical tube under the effect of a magnetic field ,International Journal of Current Research 1, (2011),105-110.

[16] S.R . Mahmoud, N.A.S.Afifi, H.M.Al-Isede,Effect of porous and magnetic field on peristaltic transport of a Jeffrey fluid, International Jornal of Mathematical Analysis 5,(2011),1025-1034.

[17] O. Manca, S. Nardini, D.Ricci A numerical stdy of nanofluids forced convection in ribbed channels, Applied Thermal Engineering 37,920120,280-292

[18] X.Wang, A.S.Mujumdar, Heat transfer characteristics of nanofluids; a review, International Journal of Thermal Sciences 46,(2007),1-19

[19] S. Nadeem, E. N.Maraj, The mathematical analysis for peristaltic flow of a nanofluid in a curved channel with compliant walls, Applied NanoSciences 4,(2014),85-92.

[20] N.S. Akbar, S. Nadeem, T.Hayat, A.A Hendi ,Peristaltic flow of nanofluid in a non-uniform tube, Heat Mass Transfer 48,(2012),481-459.

[21] C.Barton and S. Raynor S, Peristaltic flow in tubes, The Bulletin of Mathematical Biophysics 30,(1968),663-680.

[22] A.Mathur ,Performance and implementation of the Launder- Sharma low Reynolds number turbulence model, Computers Fluids 79,(2013),134-139.

[23] K.Mehmood, s. Hussain ,M. Sagheer, Numerical simulation of MHD mixed convection in aluminawater nanofluid filled squaqre porous cavity using KKl model: Effects of non-linear thermal radiation and inclined mafnetic field, Journal of Molecular Liquids 238,(2017),485-498.

[24] M. Bilal, M. Sagheer, S. Hussain, Three dimensional MHD upper-convected Maxwell nanofluid flow with nonlinear radiative heat flux, Applied Mathematics and Comptation,(2017), In Press.

[25] J. Buongiorno, Convective transport in nanofluids, Journal of Heat Transfer 128, (2006),240-250.

[26] S.Kline, Similitude and Approximation Theory, McGraw Hill,(1965).

[27] H.Douglas, De.Gerard.An Interoducion to Finite Element Analysis,Acadamic Press, (1978).New Yark.

[28] R.Hamilton, K. Crosser, Thermal conductivity of hertogenous component system, Industrial and Engineering Chemistry Fundamentals 1, (1962),187-191.

[29] S. Jan,SUS. Choi, Role of Brownian motion in the enhanced thermal conductivity of nanofluids. Applied Physics Letter 84. (2004),4316-4318.

[30] E. Efstathios, Michaelides, Nanofluidies: thermodynamics and transport properties, Springer International Publishing Switzerland.

[31] JC. Maxwell, A Treatise on Electricity and Magnetism, Clarendon Press, (1873),Oxford.

[32] RL. Hamilton, Thermal conductivity of heterogeneous two-component system, Industrial and Engineering Chemistry Fundamentals 1, (1962),187-191.

[33] EV. Timofeeva, JL.Routbort, D. Singh, Particle shape effects on thermophysical properties of alumina nanouids, Journal of Applied Physicsn106, (2009), 0143 304.

[34] K.Nowar, Peristaltic Flow of a Nanofluid under the Effect of Hall Current and Porous Medium, Mathematical Problems in Engineering, (2014).